THE DETERMINATION OF LATERAL STABILITY DERIVATIVES FOR A NAVION AIRPLANE FROM STEADY STATE DYNAMIC FLIGHT TESTING

George E. DeLong
Robert S. Moore

53

THE DETERMINATION OF LATERAL STABILITY DERIVATIVES FOR A NAVION AIRPLANE FROM STEADY STATE DYNAMIC FLIGHT TESTING

Lieutenant George E. DeLong, USN
Lieutenant Robert S. Moore, USN

Aeronautical Engineering Report No. 388
May 15, 1957

ACKNOWLEDGEMENTS

The authors wish to express their gratitude for the opportunities and facilities provided by Princeton University at the Forrestal Research Center for the undertaking of this thesis project.

The authors wish to express particular appreciation to Professor Edward Seckel, under whose supervision and guidance the project was carried out. The authors are also indebted to Mr. Enoch J. Durbin and Mr. Esteban Martinez for their aid in the instrumentation system, and to Mr. Robert F. Cooper, Mr. Barton G. Reavis, and Mr. Willson M. McCredie for their assistance in the installation of the instrumentation and their excellent maintenance of the test aircraft.

The Instrumentation Laboratory of the U. S. Naval Air Test Center, NAS Patuxent River, Maryland, contributed materially to the success of the instrumentation by their generous loan of two very fine rate gyros.

TABLE OF CONTENTS

LIST OF TABLES

LIST OF FIGURES

LIST OF FIGURES (Continued)

LIST OF SYMBOLS

A_β, A_ϕ, A_ψ	Parameters defined in Appendix A
B_β, B_ϕ, B_ψ	Parameters defined in Appendix A
b	Wing span, feet
C_L	Lift coefficient, L/qS
C_n	Yawing moment coefficient, N/qSb
C_l	Rolling moment coefficient, L'/qSb
C_y	Lateral force coefficient, Lateral Force$/qS$
C_1, C_2, C_3	Coefficient of transfer functions, defined in Appendix A
$C_{l_\beta}{}^*$, $C_{n_p}{}^*$, $C_{l_{\delta_a}}{}^*$	Stability and control derivative coefficients in equations of lateral motion, defined in Appendix A
D	Differential operation, $\frac{d(\ )}{dt}$
g	Acceleration due to gravity, feet/second^2
I_x	Moment of inertia about stability X-axis, slug-feet^2
I_z	Moment of inertia about stability Z-axis, slug-feet^2
I_{xz}	Product of inertia referred to stability axes
i	$\sqrt{-1}$
k_x	Radius of gyration about stability X-axis, feet
k_z	Radius of gyration about stability Z-axis, feet
L	Lift, pounds
L'	Rolling moment, foot-pounds
m	Aircraft mass, W/g, slugs
N	Yawing moment, foot-pounds

p or $\dot{\phi}$	Incremental rolling angular velocity about X-axis, radians/seconds
q	Dynamic pressure, $\frac{1}{2} \rho V^2$, pounds/feet^2
r or $\dot{\psi}$	Incremental yawing angular velocity about Z-axis, radians/second
S	Wing area, feet^2
s	Laplace transform variable
t	Time, seconds
V	True airspeed, feet/second
W	Aircraft weight, pounds
X, Y, Z	Aircraft stability axes
α	Angle of attack, radians
β	Angle of sideslip, v/V, radians
δ_a	Aileron control deflection, radians
δ_r	Rudder control deflection, radians
μ	Non-dimensional mass parameter, $m/\rho Sb$
ρ	Air density, slugs/feet^3
τ	Non-dimensional time parameter, $m/\rho SV$
Φ	Phase angle, radians
ϕ	Angle of roll, radians
ψ	Angle of yaw, radians
ω	Angular frequency, radians/seconds

The lateral stability derivatives are expressed by subscript notation as, for example:

$$C_{l_\beta} = \frac{\partial C_l}{\partial \beta} \quad , \quad C_{n_p} = \frac{\partial C_n}{\partial \left(\frac{pb}{2V}\right)} \quad , \quad C_{n_r} = \frac{\partial C_n}{\partial \left(\frac{rb}{2V}\right)}$$

Phase angles are also indicated by subscript notation, as the phase angle between the input rudder deflection and the output side-slip angle would be:

$$\Phi_{\beta_{\delta_r}}$$

SUMMARY

This investigation was performed to determine the feasibility of obtaining lateral frequency response and stability derivatives utilizing the forced oscillation technique. Tests were conducted in a North American Navion at one altitude, airspeed and gross weight condition.

Both rudder and ailerons were oscillated sinusoidally with a simple mechanical oscillator and aircraft responses were telemetered and recorded on magnetic tape. A technique was developed for eliminating distortion of the input sine wave by utilizing a low frequency band pass filter in the reduction of flight data. Frequency responses were determined for ϕ , ψ , and β for both the rudder and the aileron oscillations; and these were used to determine the aircraft's stability derivatives. Frequency responses were calculated from the experimentally determined derivatives and were compared with the actual frequency responses to illustrate the accuracy of the method employed to extract the stability derivatives.

The methods employed proved entirely feasible for this aircraft at the single flight condition and apparently were applicable to many current production aircraft. The frequency responses showed little random error, and the responses calculated from the experimentally determined derivatives closely matched the actual responses.

INTRODUCTION

The design of modern high speed aircraft and the automatic control systems with which nearly all are equipped requires an accurate evaluation of their response characteristics. In the early design stages the only method available to the designer involves the estimation of the aircraft's stability derivatives and the solution of the assumed equations of motion. Because of the inherent difficulties involved in the analytic determination of stability derivatives, large errors may be present in the derived response characteristics. Dynamic flight testing of the prototype aircraft to accurately determine its stability derivatives and the coefficients of its transfer function is becoming increasingly important.

Dynamic flight test data is usually obtained by one of two methods. The most popular of these involves the determination of the transient response of the aircraft to known control inputs. While the data thus obtained is, in itself, not in the best form for analysis, the recent development of efficient computing machines has made it possible to convert such a transient response to frequency response form where it may be more readily analyzed. The second method involves the direct determination of the aircraft's frequency response by the steady state forced oscillation technique. While considerably more flight time is required in this method, data reduction is greatly simpli-

fied; and good results may be obtained without the use of automatic computers.

The determination of an aircraft's lateral frequency response by the forced oscillation technique may be accomplished by oscillating either of the lateral controls with a sinusoidal forcing function while keeping the other locked. From simultaneous recordings of the aircraft responses in $\dot{\phi}$, $\dot{\psi}$ and β and the control inputs on separate time traces, it is possible to determine amplitude ratios and phase angles for each response over a range of oscillation frequencies for the steady state condition. From these amplitude and phase spectra it is, in theory, possible to determine from either the aileron or rudder data all the aircraft's aerodynamic derivatives, except of course the control derivatives for the locked surface, providing the weight and moments of inertia of the aircraft are known. In practice, however, it is frequently difficult to determine all the derivatives accurately since some of them have little effect on the frequency response and thus are difficult to determine from it.

While considerable effort has been expended on this type of testing, especially at the Cornell Aeronautical Laboratory, the accurate determination of derivatives without harmonic analysis of the time traces has required very pure sinusoidal control inputs. This requirement has led to complicated instrumentation which has made the method applicable only to research type testing.

This investigation was conducted to determine the applicability of the method to more simplified testing techniques utilizing a simple mechanical oscillator, telemetering equipment for data recording, and an ultra-low frequency band-pass filter to eliminate sine wave distortion. The flight tests were conducted in a North American Navion at the Forrestal Research Center, Princeton University, during the winter and spring of 1957.

EQUIPMENT

Test Airplane

The test airplane was a North American Navion, which is an all metal, four place, low wing, single engine airplane. The Navion is equipped with a Continental E-185 engine, rated at 185 HP at 2300 RPM and 29 inches of MP, at sea level. The wing is unswept, and the tail configuration conventional. The control surfaces are all of beaded skin construction, and have no trailing edge extensions. Trim tabs are located on the elevator, aileron, and rudder.

The test airplane was modified by the removal of the two rear cockpit seats to provide space for the test instrumentation. The test airplane had a gross weight of 2870 pounds with full service, pilot and co-pilot, and all test equipment.

A three view drawing of the Navion is shown in Fig. 1 and the general specifications of the test airplane are tabulated in Table I. Fig. 2 is a photograph of the test airplane.

Power Supply

Power available for the instrumentation in the test airplane included both 12 and 28 volt direct current supplied by a 28 volt engine driven generator and two 12 volt batteries connected in series. A 500 VA voltage and frequency controlled inverter was installed behind the co-pilot's seat to provide 115 volt, 400 cycle, three phase alternating current power to the gyros and telemeter transmitter.

Considerable effort was expended in obtaining an inverter which could be frequency controlled, since it was very important that the three phase power to the rate gyros be constant at the calibration frequency of 400 cycles.

A circuit diagram of the aircraft 28 volt system and the inverter system is shown in Fig. 3.

Aircraft Instrumentation

Standard aircraft instruments were used to determine indicated airspeed and altitude. Measurement of the following quantities was required: sideslip angle, yaw rate, and roll rate with respect to wind or stability axes, and aileron and rudder position angles. In choosing the type of components needed to measure the above quantities, an attempt was made to utilize instrumentation compatible with the telemetering equipment. For this reason, the transducers selected were of the potentiometer type, not only because they were capable of providing signals of sufficient magnitude, but also because their excitation source readily provided zero and full scale reference voltages.

In view of some past history of various amounts of coupling between the response of the aircraft and certain of the instrumentation components in this type of flight testing, considerable attention was given to choosing transducers with satisfactory frequency response characteristics in order to avoid correction of response data for the dynamics of the recording instruments. In general, it was desirable

that the natural frequencies of the rate gyros and the sideslip vane be large as compared to the expected forced oscillation frequencies of the aircraft.

Sideslip angle was sensed by a light vane mounted on a boom approximately one maximum fuselage diameter ahead of the left wing tip. The moment of inertia of the vane was very low, and no gearing was introduced in the linkage in order to keep the natural frequency and damping within acceptable limits. An Electro-Mechanical Laboratory ultra-low torque potentiometer with .008 inch-ounces of friction torque was obtained for use with the sideslip vane.

In order to reduce boom resonance, which had been experienced in previous tests with the Navion, the boom was stiffened by three angle strips equally spaced around the periphery, and running the full length of the boom. The sideslip vane and the boom are shown in the assembled condition in Fig. 4.

Aileron and rudder angle were measured by 10,000 ohm Model 5301 single turn Helipot precision potentiometers. Due to the nature of the differential aileron system of the Navion, it was not considered desireable to pick off aileron angle at the aileron itself. Accordingly, the pickoffs were made from the control cable movement just inboard of the right aileron. A position close to the aileron was chosen in order to avoid the effects of cable stretch. The rudder deflection potentiometer was mounted on the bottom of the rudder and was actuated by a cable under spring tension.

The measurement of yaw and roll rates was accomplished with type 3612 Giannini rate gyros. This type of gyro operates on a power supply of 115 volt, 400 cycle, three phase AC to the motor, and 115 volt single phase AC to the heaters. The transducer is of the potentiometer type, with a DC resistance of 5250 ohms. These gyros were obtained on loan from the Instrumentation Laboratory of the U. S. Naval Air Test Center, NAS Patuxent River, Maryland.

Oscillating Mechanism

Design of the control driving mechanism was based on the following criteria: (a) The system must generate a sinusoidal output of controllable frequency which may be applied to either the rudder or the aileron control; (b) The driving link for the driven control, and the locking mechanism for the undriven control must each include a quick disconnect, not subject to binding when under load; (c) Driving and locking links must include a trim adjustment; (d) Inter-unit rigidity and close tolerances are required due to the cyclical varying load; and (e) The unit must be compatible with the power and space limitations of the Navion.

These conditions were met in the following manner. The rotation of a 400 cycle, 1/2 HP DC motor was converted to a pure sinusoidal translational motion by a scotch yoke, with suitable intermediate gearing. The driving rod to the rudder could be disconnected from the scotch yoke plate and bolted to the mounting plate to provide a positive

rudder lock. The rod from the scotch yoke plate was fitted inside a tube from the rudder. By use of a large handled set screw the rod and tube could be rigidly locked at any desired trim position, and quickly unlocked without possibility of binding. The aileron drive was obtained by leading light aircraft control cable around pulleys from the horizontally translating shaft of the scotch yoke to a set of vertically translating turnbuckles, from which a chain drove a sprocket wheel mounted on the control column. The sprocket was secured to the control column by a large handled set screw arrangement which allowed aileron trim adjustment and a quick disconnect. To lock the ailerons, the drive was opened at the turnbuckle and a cable bolted to the base plate substituted for the driving cable.

The motor, gear box, and driving and locking unit was built up on one large section of 1/4" aluminum plate, which provided a very rigid base. The complete mechanism could be installed or removed as a unit, the plate being bolted to extrusions riveted to the siffeners under the deck on the starboard side of the cockpit. In-flight shifting from the aileron drive to the rudder drive involved about five minutes.

Control of the driving motor was obtained by the use of an amplidyne mounted behind the co-pilot. Through control of the field of the amplidyne, whose output provided the armature current to the driving motor, any speed from zero to maximum rated, including reversing, could be obtained. Indication of the operating frequency was not directly

available in the cockpit, but could be obtained approximately from a calibrated voltmeter across the amplidyne signal circuit. At the lower frequencies, the torque (proportional to the armature current) became marginal, and was evidenced as a distortion to the sine wave of the driven control as the aerodynamic load varied with control displacement. A worm and gear was incorporated in the gear box to obtain irreversibility between the motor and the control surfaces, but the variation of the frictional load on the worm was sufficient to cause this low frequency distortion. The aircraft instrumentation is shown in Fig. 6 and a close up of the oscillating mechanism is shown in Fig. 7.

Signal Circuit Design

The telemeter transmitter was designed to accept voltages from the transducers from zero to five volts. It was thus desirable for the full scale voltages on the potentiometers to be maintained at five volts. Variations in this full scale value were permissable, providing that the variation on all the potentiometers was the same, since the telemeter corrected all voltages to a percentage of the full scale reference voltage. The potentiometer used in the sideslip vane was a 360 degree single turn model, and, since only 40 degrees of variation in sideslip angle were expected, it was necessary to apply 45 volts excitation to this potentiometer in order that its output might have a five volt variation. The use of a 45 volt DC signal circuit supply was thus dictated. It was also desirable to maintain the signal voltage to the other potentiometers at five volts

and introduce a biasing circuit to provide a variation of sideslip output voltage from zero to five volts rather than a five volt variation about some intermediate voltage.

The signal circuit design based on the preceding requirements is shown in Fig. 5. The essential element of the circuit is the bias supply voltage potentiometer, pot "A". With the sideslip vane against the stop in one direction, pot "A" was adjusted so that the output voltage of the sideslip pot was zero. The vane was then deflected to the opposite stop, and the output voltage of the sideslip pot was recorded. This value was slightly less than five volts. Pot "B" was then adjusted to bring the full scale reference voltage, and thus also the voltage in the remaining signal circuits in agreement with the full scale sideslip voltage. The procedure was repeated two or three times as necessary, in order to nullify any loading on the system. Once the final adjustment was made, the zero to full scale voltage for each quantity to be measured was exactly the same, and small variations in signal voltage produced the same variation for all circuits. Pots "A" and "B" were locked and required no further adjustment for the remainder of the project.

During the initial flight and transmission tests, considerable AC ripple was found to enter the DC signal voltages, very likely from the 400 cycle inverter. Condensers "C" and "D" in Fig. 5 were installed, and were found to reduce the ripple to a negligible value.

Telemeter System

The telemeter unit was of the pulse width type and was designed and built by the Applied Science Corporation of Princeton (ASCOP). This unit was the key element in the instrumentation of this project. The basic functional components of this pulse width system are transducers (all of the potentiometer type); a time division multiplexer, or commutator; an electronic coder, or keyer to put the intelligence into pulse form; an RF transmitter; and ground station equipment for receiving, decoding, and recording the data in usable form.

The airborne component of the system is designated the ASCOP D Series PW Multicoder, and the ground station equipment the ASCOP M Series PW Ground Station.

A unique feature and very great advantage of pulse width data systems is that, due to the multiplexing or time sharing operation, all data channels traverse the same path during transmission. Since zero and full scale references are transmitted with the data, this results in a calibration signal, effective for all channels, being transmitted 20 times each second. These calibration signals allow the removal of almost all of the system error, with the exception of errors introduced in the instrument pickups and the mechanical switch, and they make possible the use of this telemetering system in tests of long duration and varying environmental conditions.

Magnetic Tape Recorder

An Ampex Model 309C dual track three speed tape recorder was an integral component of the ground station equipment, and provided a convenient means for recording, storage, and playback of the standard pulse width modulated data. Provisions were also included for placing voice transmissions directly on the magnetic tape from either or both the aircraft and the ground station.

Data Recorder

Qualitative analysis of the flight data during the actual flights and quantitative analysis of the recorded signals was made on a Sanborn Model 154-100D four channel recorder. This instrument had a very high natural frequency (42 cps), and the low frequency response was flat to zero cps. Different paper speeds and variable gain were possible and permitted expansion of the time trace and amplification of the signal to nearly any desired value.

Filter

In order to study the response of the aircraft to a true sinusoidal driving function, all forcing functions and the corresponding responses were filtered to remove all but the fundamental frequency. The filter employed was the model 330-A KROHN-HITE Ultra-Low Frequency Band-Pass Filter. This is an adjustable filter whose gain is unity in the pass band and drops outside the pass band at the rate of 24 db per

octave. The filter combines a high pass filter and a low pass filter, each of which may be continuously tuned from 0.02 to 2,000 cps. Since the filter will handle an input signal of only up to 10 volts rms without overloading, a voltage divider was applied to the telemeter output, which had a full scale range of up to 100 volts. For this application the filter was used as a narrow pass band with the high and low dials set at the same frequency. Used in this manner, the filter did not alter the relative amplitude or phase relationships between the input and the output at a specific frequency.

A photograph of the ground instrumentation is shown in Fig. 8.

Instrument Calibration

Six items required calibration in the instrumentation system. These were the two rate gyros, the two control deflection potentiometers, the sideslip vane potentiometer, and the signal voltage to the amplidyne which was roughly a measure of the frequency of control oscillation. The aircraft altitude and airspeed indicating systems were not calibrated because previous calibrations indicated that the errors here were negligible for the conditions of this investigation.

The two rate gyros were calibrated on a pendulum which consisted of a 3/4" diameter aluminum shaft and a 12" diameter instrument pan. The pendulum, the overall length of which was 121.75" was pinned to the overhead truss structure in the Forrestal hangar. A scale was mounted with brackets on a small table in such a way that displacement

of the pan from its rest position could be measured. The gyros were mounted one at a time on a wooden base plate which was clamped to the pendulum pan, and their potentiometer outputs were connected to a Brush Recorder. The pendulum was displaced from its rest position and allowed to swing freely. Since there was an excessive amount of friction in the system, swing amplitudes were measured on two successive swings in the same direction and averaged. The two maximum voltages recorded during the swing were also averaged and the maximum rate attained during the swing was determined from the following relation:

$$\dot{\theta}_{max} = \frac{d}{\ell} \frac{360}{P}$$

where P was the natural period of the pendulum whose measured value from the trace on the Brush recorder was 3.33 sec., l was the length of the pendulum, and d was the average maximum displacement of the pan from its rest position. The pendulum was allowed to swing until once again at rest with readings taken, as described above, over the entire range of gyro rates. The angular rate gradient of both gyros was found to be linear and equal to .610 degrees/sec. per percent full scale potentiometer voltage. The gyro calibration curves are shown in Fig. 9. It was found that the gyros were very sensitive to the frequency of the 400 cycle supply voltage and as a result great care was taken during calibration and also during the actual flight test program to maintain the frequency of the supply at exactly 400 cycles per second.

The control deflection potentiometers were calibrated by measuring the resistance between the output terminals over the full range of control deflections. The actual control deflections were measured with a vernier protractor capable of accuracy to 0.1 degree. The rudder deflection gradient was found to be linear and equal to .405 degrees per percent full scale potentiometer voltage. The Navion aircraft is equipped with differential ailerons and it was expected that the aileron calibration would therefore be non-linear. However, using average aileron angle, it was found that over the small deflection range of +10 to -10 degrees desired during the flight test program the aileron deflection gradient was linear and equal to .1933 degrees per percent full scale potentiometer voltage.

The sideslip vane potentiometer was calibrated in the same manner as the control deflection potentiometers, using a protractor and measuring the resistance between the output terminals with an ohmmeter. The calibration curve is shown in Fig. 10. The sideslip gradient was found to be linear and equal to .468 degrees per percent full scale potentiometer voltage.

The telemeter equipment corrected its output to percent full scale voltage and since full scale voltage on all the potentiometers varied by the same increment as the reference voltage for small fluctuations of the latter value, it was unnecessary to calibrate the potentiometers through the telemeter equipment.

The speed control on the oscillating device was calibrated roughly in flight by timing the frequency of control oscillations and recording

the voltmeter reading across the control field of the amplidyne generator. This speed control was used only to obtain order of magnitude settings, the actual frequency of any particular oscillation being determined from the trace on the Sanborn Recorder.

Careful consideration was given to the possible errors which might be introduced in the data by the dynamics of the recording instruments. The natural frequency of the rate gyros was 17 cycles per second and their damping ratio was between .45 and .7. The natural frequency and damping ratio for the sideslip vane were experimentally determined in flight to be 15.44 and 0.081 respectively. Since the natural frequency of the aircraft was approximately 0.4 cycles per second and the maximum forced oscillation frequency was not expected to exceed one cycle per second, the attenuation of the signals due to the dynamics of the instruments was effectively zero. While a small error in phase angle measurement was introduced at the higher frequencies, it was considerably smaller than the reading accuracy with which phase angle could be determined from the data, and thus was not considered in the reduction of flight test data.

FLIGHT TEST PROCEDURE

In this investigation, frequency response was measured at the single flight condition of 5000 ft. density altitude, 129.6 mph true airspeed, and 2870 lbs. gross weight. Each test was commenced at steady level flight with the amplidyne control set at zero speed, the oscillating mechanism exactly centered to its mid position, and the lateral controls locked in this trim position. The run was then initiated by setting the speed control and allowing steady state conditions to become established. The necessity for driving the lateral controls about the exact trim position was so great that the lock-on system to a moving oscillator, as employed in a somewhat similar longitudinal study (Ref. 1) was not feasible. In spite of the great care exercised to center the oscillations about a straight and level flight path, practically every run was ultimately terminated by the excitation of the spiral mode. At this time the rapid unlocking features in the mechanical system design were most appreciated.

In setting the speed control, an approximation to the desired frequency could be obtained by the use of a voltmeter across the amplidyne control field calibrated to read frequency. The relatively short duration of each run did not permit fine adjustments to obtain a specific frequency, so several runs around a desired frequency (primarily near the dutch roll) were employed. In addition, it was found that the low

frequency runs were best started by going rapidly to a high frequency, and then coming down to the desired frequency. Otherwise, the response to the slow initial deflection drove the aircraft so far into the spiral divergence that the subsequent control reversal was insufficient to establish an oscillation about a straight flight path. Although it had been expected that all controls except the driven one would be locked during a run, it was found that slight elevator movements were required to maintain a constant airspeed throughout the run, particularly during oscillations of the rudder.

RESULTS

Data Reduction

The quantities measured during the flight test program were δ_a or δ_r, β, $\dot{\phi}$, and $\dot{\psi}$. These four quantities were telemetered to the ground station, recorded on magnetic tape, and simultaneously plotted on the Sanborn Recorder. This raw data had noise and distortion superimposed on the fundamental sinusoidal driving frequency. An example of such a record is shown in Fig. 11. In order to study the response of the aircraft to only the fundamental of the driving frequency, a KROHN-HITE Ultra-Low Frequency Band-Pass Filter was used to filter both the driving function and the aircraft responses. From the original record of the raw data the fundamental frequency for a particular run could be determined with sufficient accuracy to establish the high and low settings for the band pass filter. With the filter thus set to pass only the specific frequency, all four quantities were successively played from the magnetic tape through the telemeter receiver (converting the pulse width coding to a varying voltage output), thence through the filter to the Sanborn recorder. As each quantity was being filtered and recorded, an unfiltered trace of the forcing function was also placed on this new record to act as a time reference. The results of this time and recorder paper consuming process were four sinusoidal records of the measured quantities, each with a common unfiltered time reference. Fig. 12 shows an example of such a filtered record with the

unfiltered forcing functions matched for each response. From these matched responses the amplitude ratios and phase angles relative to the driving quantity could be determined. Since the settings on the filter and the recorder were not altered during the filtering of a given frequency, any amplitude attentuation or phase shifting was applied equally to all four quantities. The gain of the recorder was initially set for each frequency to accommodate the quantity with the greatest amplitude, such that this quantity would utilize almost full scale on a recorder paper channel. By using this technique, and increasing the paper speed for the higher frequencies, a rather accurate determination of the amplitude ratios and phase angles was possible.

The quantities ϕ and ψ were determined from the records of $\dot{\phi}$ and $\dot{\psi}$ by integration. This was readily performed by dividing by ω and subtracting 90° from the phase angle, since the response was sinusoidal. The magnitude of each response was divided by the magnitude of the forcing function and the appropriate scale factors were applied to give the desired amplitude ratios. Since the sideslip vane was not located at the c.g. of the aircraft an additional correction to the β response was required. This correction was a function of the distance of the sideslip vane from the c.g. of the aircraft and is given by the following relation: $\Delta\beta = -.0274\,\dot{\psi}$
The final frequency responses were tabulated in Tables II and III and were plotted in Figs. 13-18 and labeled "experimental."

Also plotted on the appropriate graphs in Figs. 13-18 were frequency response curves denoted as "theoretical." These curves were the result of an initial study of the Navion airplane based on lateral stability derivatives determined from previous tests, such as described in Ref. 2, or from theoretically determined derivatives. These initial "best guess" derivatives are tabulated in Table IV, and were used as a rough check on the results, as well as the basis for the initial system design.

Determination of Derivatives

Ref. 3 develops a method for extracting stability derivatives from frequency response data for the lateral case. The method involves the application of the vector technique to the three linear equations of lateral motion to separate them into six equations. The vector responses are resolved parallel and perpendicular to the control deflection vectors. The perpendicular resolution eliminates the control deflection derivatives in one of the two equations derived from each basic equation and thus permits solution of the aerodynamic derivatives separately. The development of these equations is shown in Appendix A. The method of least squares is then applied to the data for each of these equations to yield lateral stability derivatives.

Although the method of least squares is probably the best way to eliminate random error, it is not readily applicable to hand calculation

techniques. Automatic computing facilities were not available here, and since time was limited, it was decided to use the simpler method of averages in conjunction with the vector equations developed in Ref. 3 to determine the lateral stability derivatives of the Navion. The K notation of Ref. 3 was modified to a starred derivative notation for greater clarity. This notation is defined in Appendix A. The method of averages, as described in detail in Ref. 4, is also outlined in Appendix A.

The components of the responses along and perpendicular to the control deflection axis are defined in the form A+iB with the appropriate subscripts. Formulas for the determination of the responses and their derivatives in this form are given in Appendix A.

The two equations developed from the basic side force equation by the vector technique are equations (13) and (14) in Appendix A. The equation describing the relation between the components perpendicular to the control deflection axis was:

$$(13)\quad C_{y\beta}^{*} - C_{L}^{*} B\phi = -\omega (A_{\beta} + A_{\psi})$$

Since the only unknown was $C_{y_\beta}^{*}$ it was possible, in theory, to determine its value from the responses to either an aileron or rudder forcing function at a single frequency. Since the responses in yaw and sideslip were greater for a rudder input, it was felt that the rudder data would give a better solution for $C_{y_\beta}^{*}$. In order to eliminate random error

the responses at 12 selected frequencies were taken from the faired rudder curves. The summation of the 12 equations determined from these 12 points gave one average equation, from which the value of $C_{y_\beta}{}^*$ was determined. This gave a value of C_{y_β} of -0.591. The same technique using aileron data resulted in a positive value for C_{y_β}, which was, of course, impossible. Ref. 3 mentions that the accurate determination of C_{y_β} may be difficult from this equation, since it involves the sum of the yaw and sideslip components, which are nearly equal but opposite in sign. The authors of Ref. 3 recommend obtaining lateral acceleration data and using a modified side force equation to avoid this condition. The large responses in yaw and sideslip to rudder inputs tended to minimize this condition, but the determined value of C_{y_β} was nevertheless subject to considerable error.

The equation describing the relation between the components parallel to the control deflection axis and therefore including the derivative, $C_{y_{\delta r}}{}^*$, was:

$$(14)\quad C_{Y_\beta}{}^* A_\beta - C_L{}^* A_\phi = C_{Y_{\delta_r}}{}^* + \omega(B_\beta + B_\psi)$$

Using the previously determined value for $C_{y_\beta}{}^*$ in an average equation for the 12 selected points yielded a value for $C_{y_{\delta r}}{}^*$. This gave a value for $C_{y_{\delta_r}}$ of 0.206. The accuracy of $C_{y_{\delta_r}}$ was clearly dependent on the correctness of C_{y_β}, and was, in addition, subject to small differences between yaw and sideslip components. $C_{y_{\delta_r}}$ was therefore of doubtful reliability.

The vector technique gave equations (15) and (16) of Appendix A from the basic roll equation. The relation between the components perpendicular to the control deflection axis was:

$$(15)\quad C\ell_\beta^* B\beta + C\ell_p^* \omega A\phi + \frac{I_{xz}}{I_x}\omega^2 B\psi - C\ell_r^* \omega A\psi = \omega^2 B\phi$$

Since I_{xz} was very small compared to I_x the term $\frac{I_{xz}}{I_x}$ was assumed to be zero. Solution for the three unknowns required three equations. The 12 frequency points from the aileron data were now grouped to include four frequencies below the dutch roll, four near the dutch roll, and four above the dutch roll, and average equations were determined for each group by adding the appropriate coefficients. Solution of these equations for $C_{l_\beta}{}^*$, $C_{l_p}{}^*$, and $C_{l_r}{}^*$ were converted to C_{l_β}, C_{l_p}, and C_{l_r}, which were -0.0505, -0.436, and 0.0390, respectively. In the solution of these equations it was found that an accurate determination of C_{l_r} was difficult, since the solution involved a small difference between large quantities; and small errors were magnified many times. An attempt was made to carry greater accuracy in the solution than the data actually warranted, but of course this procedure, while required to give any solution at all, could not give an accurate solution for C_{l_r}. This condition was not surprising, since it is well known that the cross derivatives are difficult to determine from this sort of data.

Solution of the same equation using a grouping of points from the

rudder data should have given the same derivatives as previously determined from the aileron data. When this solution was attempted, however, it was found that the simultaneous equations were ill-conditioned. This arose from the fact that β and $\dot{\phi}$ varied in nearly the same manner over the entire frequency range, both in phase angle and magnitude. Additional frequency points were taken and various groupings were tried in an attempt to eliminate this difficulty, but all were unsuccessful. Ref. 3 suggests a possible method of avoiding the difficulty by eliminating the cross derivative coefficient by resolution of the vectors along the ϕ axis, instead of along and perpendicular to the control deflection axis. This was attempted, but solution of the modified equation was still impossible.

It was felt that the rudder data was slightly better than the aileron data, due to refinements in the flight test technique as the program progressed, and it was therefore highly desirable to include the rudder data in the solution for the roll derivatives. The solution of the aileron equations gave a value of $C_{l_p}{}^*$ which was felt to be quite accurate, since it was in close agreement with theory and previous experimental results. This value was assumed known in the rudder equations for the rolling motion, and the two remaining derivatives $C_{l_\beta}{}^*$ and $C_{l_r}{}^*$ were determined by taking two groups of six frequency points each and arriving at two equations in the two desired unknowns. The values determined for C_{l_β} and C_{l_r} were -0.0513 and 0.119 respectively.

It was interesting to note that the value of C_{l_β} determined in this manner was nearly the same as that determined from the aileron data, and the doubtful derivative, C_{l_r}, was nearer the theoretically determined value. The derivatives determined in this manner were arbitrarily chosen as the final values, since the authors felt that they represented the best possible combination of all the experimental data.

The relation between the components parallel to the control deflection axis was:

$$(16)\quad C\ell_\beta^* A_\beta - C\ell_p^* \omega B\phi + \frac{I_{xz}}{I_x} \omega^2 A\psi + C\ell_r^* \omega B\psi - C\ell_{\delta_r}^* = \omega^2 A\phi$$

Using the previously determined values of C_{l_β}*, C_{l_r}*, and C_{l_p}* and utilizing one average equation based on all 12 frequency points from the rudder data permitted solution for $C_{l_{\delta_r}}$*, which gave a $C_{l_{\delta_r}}$ of 0.0128. Similarly, solution of the same equation using the aileron data gave $C_{l_{\delta_a}}$*, which resulted in a value for $C_{l_{\delta_a}}$ of -0.108.

Expressing the basic yaw equation in vector form resulted in equations (17) and (18) of Appendix A. For the components perpendicular to the control deflection axis the relation was:

$$(17)\quad -C_{n_\beta}^* B_\beta - C_{n_p}^* \omega A\phi + \frac{I_{xz}}{I_z} \omega^2 B\phi + C_{n_r}^* \omega A\psi = \omega^2 B\psi$$

Because of the basic similarity between the equations for the yawing

and rolling motions, the unknowns in equations (15) and (17) have the same numerical coefficients, with only the constant term differing. Because of this, rapid solution of the three average equations for the yawing motion was possible using the same grouping of frequency points from the responses to aileron oscillations. This gave values of C_{n_β}, C_{n_p}, and C_{n_r} of 0.0771, -0.129, and -0.0841, respectively. The same difficulty existed here in the determination of C_{n_p} as had previously existed in the determination of C_{l_r}.

Because the numerical values of the coefficients of equation (17) were the same as those of equation (15), the three simultaneous equations for the yawing motion derived from the rudder data were also ill-conditioned for solution. The method applied to solve equation (15) using an apparently accurate value of C_{l_p} could not be applied in this case, because both C_{n_β} and C_{n_p} as determined from the aileron data were felt to be doubtful, since they were not in agreement with either theory or the results contained in Ref. 5. In this case, final solution was effected by solution of a set of simultaneous equations, two of which were determined from the aileron data at frequencies near and above the dutch roll, and the third representing the average of all the rudder data. This approach appeared legitimate since each equation in the set was independent of the type of forcing function. This particular choice of equations resulted from the opinion of the authors that the aileron data was better at higher frequencies and that inclusion

of the generally more reliable rudder data was desirable. It should be emphasized that this particular choice was peculiar to this experiment. Solution of these equations gave values for C_{n_β} , C_{n_p} , and C_{n_r} of 0.0895, -0.106, and -0.0908 respectively.

The equation relating the components parallel to the control deflection axis for the yawing motion was:

$$(18)\quad -C_{n_\beta}^{*} A_\beta + C_{n_p}^{*} \omega B\phi + \frac{I_{xz}}{I_z} \omega^2 A\phi - C_{n_r}^{*} \omega B\psi - C_{n_{\delta r}}^{*} = \omega^2 A\psi$$

Using the previously determined values of $C_{n_\beta}^{*}$, $C_{n_p}^{*}$, and $C_{n_r}^{*}$ and utilizing all 12 frequency points from the rudder data permitted solution for $C_{n_{\delta r}}$ *, which gave a $C_{n_{\delta r}}$ of -0.0673. Similarly solution of the same equation using the aileron data gave $C_{n_{\delta a}}$ *, which resulted in a value for $C_{n_{\delta a}}$ of 0.00376.

The final derivatives determined in this investigation are tabulated in Table IV. This table also contains the original theoretically determined derivatives, and the derivatives determined for the same aircraft by an analog computer solution as outlined in Ref. 5.

In order to check the accuracy of the method used to determine the aircraft's stability derivatives, the transfer function coefficients based on them were determined as outlined in Appendix A, and from these the frequency responses were calculated. The experimental transfer functions are tabulated in Table V, and the frequency responses based on them are shown in Fig. 19-24.

DISCUSSION

Dynamic flight testing is becoming increasingly important with the advent of high speed high altitude aircraft because the aircraft designer is more concerned than ever before with the accurate determination of stability derivatives and the associated transfer functions. Although transient methods are the most popular at the present time, it was felt that if the instrumentation requirements of steady state dynamic flight testing could be reduced and the necessity for absolutely sinusoidal control inputs without the added requirement of harmonic analysis could be eliminated the forced oscillation technique for determining frequency response and thus stability derivatives and transfer function coefficients could still be used to advantage under certain circumstances. It was the purpose of this investigation to examine the possibility of obtaining adequate frequency response with relatively simple instrumentation, and if possible to eliminate the necessity of harmonic analysis due to distorted sinusoidal inputs.

Since investigation of the methods involved was of primary concern here, flight tests were conducted at only one altitude, airspeed, and gross weight condition, although it should be emphasized that in any actual flight test program to determine derivatives, all of these conditions should be varied over the operating range of the aircraft.

Before the design of the instrumentation system could be accomplished a prediction of the results based on theoretically determined

derivatives and control gradients was required. Obviously the experimental data had to include frequencies on either side of the dutch roll with frequencies at the dutch roll being of primary interest. Previous investigations of the lateral dynamic stability of the Navion indicated that the period of the dutch roll was between 2 and 3 seconds. An analysis based on the best available derivatives, some calculated theoretically from Ref. 6 and others taken from Ref. 2 and 7 was performed. This indicated that the period of the dutch roll was about 2.4 seconds. Theoretical frequency responses to both rudder and aileron forcing functions were calculated and these served to design the instrumentation system.

It was decided to design the oscillator to cover frequencies between 0.5 and 10 radians per second. The upper limit proved higher than necessary and better results would have been obtained if the design had limited the upper frequency to 5 radians per second. This upper limit was found to be well above the dutch roll frequency and oscillations at higher frequencies produced only negligible responses. Examination of the control deflections necessary to produce recordable responses without exceeding the linear limit of the equations and the control gradients led to the decision to use a $\frac{1}{2}$ H.P. motor and an amplidyne to control its armature current. Early experimentation with a mechanical variable reduction gear indicated that this method was unsatisfactory.

Ref. 1 recommends a careful preliminary study of the dynamics of the recording instruments since, if their natural frequency is not much larger than the natural frequency of the aircraft, large errors arise which must be corrected for. This was done, and it was found that the natural frequency of the rate gyros and sideslip vane were such that the attenuation of their signal outputs was effectively zero and that the phase shift introduced was less than 0.5^{o}. Since other errors in phase angle measurement were expected to be of considerably greater magnitude, no attempt was made to correct for the dynamic response of the recording instruments.

The instrumentation system based on the results of the above calculations proved completely adequate with the exception of the oscillator. It was found that since the output torque was directly proportional to the armature current of the motor the torque at low frequencies and thus low armature currents was insufficient to produce anything approaching a pure sinusoidal control motion. Consideration was given to changing the reduction gear ratio and thus providing more torque at low frequencies, but this was discarded because of time requirements. The gyros were properly utilized, and their limitations were never exceeded; and the original estimates of the control deflections required to produce the desired responses proved accurate, making major modification of the original instrumentation unnecessary.

Several difficulties were encountered during the flight test program.

The initial flights were conducted with the rudder locked and with the ailerons driven by the oscillator. At oscillation frequencies well above the dutch roll the steady state condition was rapidly reached and satisfactory data could be obtained before the spiral mode was excited. At frequencies near the dutch roll the spiral mode was frequently excited before the steady state condition was reached necessitating termination of the run before any data could be obtained. At frequencies below the dutch roll the initial control deflection was sufficient to excite the spiral mode, and no data at all could be obtained. After some experimentation it was found that most of this difficulty could be eliminated by starting the oscillations at a high frequency and then reducing the frequency to the desired value, and this procedure was adopted in all subsequent flight tests both for aileron and rudder oscillations. During the runs involving aileron oscillations there was very little indication to the pilots when the dutch roll frequency was being approached, and it was not until the data was reduced that it could be seen that the responses peaked at this frequency. During the runs involving rudder oscillations, however, the responses became quite violent at the dutch roll and apparently very sensitive to airspeed. During the first rudder run at the dutch roll frequency the airspeed control was poor, and as speed decreased by as little as 6 mph the responses decreased in a very noticeable manner. As speed was increased to the desired value by retrimming the elevator, the resonant condition was again reached

and the responses became large. A similar variation was noted with an increase in airspeed over the desired value, but the effect was not as pronounced. The difference between the effects was explained by reference to the final response curves which show a rather flat top at the dutch roll frequency. A decrease in velocity corresponds to an increase in τ and this in turn corresponds to a decrease in the dutch roll frequency. Since the actual frequency of the oscillations was maintained constant, the operating point at the decreased velocity was actually above the dutch roll. Since the experimentally determined response curves fall off more rapidly above the dutch roll than below it, the condition was satisfactorily explained. Because of the violence of the responses near the dutch roll and their sensitivity to airspeed great care was necessary to keep the speed at its desired value, and runs where speed control was poor were discarded.

Ref. 1 discusses some difficulty in the design of satisfactory control locking and trim devices for the oscillation mechanism. The original design accomplished here utilizing the recommendations of Ref. 1 proved highly successful and no difficulty was encountered either in obtaining proper trim or in releasing the oscillator or the locked control surface when the attitude of the aircraft made this necessary.

While it was felt in the original design that a measure of the control field voltage to the amplidyne would serve as a satisfactory indication of the frequency of oscillation, it was found that this assumption

was not wholly justified. A rough determination of frequency could be made from this voltage reading, but because of residual magnetism in the control field of the amplidyne, the desired accuracy could not be attained. Precise frequency determination for data analysis was made from the recorded traces, but since a fairly accurate knowledge of frequency in the cockpit during the flight testing was desirable it is recommended that in subsequent tests of this nature a tachometer generator be incorporated on the driving motor.

In the analysis of the data at low frequencies it was found that, although the inputs were not purely sinusoidal, the steady state condition was rapidly reached. Harmonic analysis of both the responses and the forcing function was considered but was discarded as being too time consuming. Since all the data had been recorded on magnetic tape, a technique of filtering both the forcing function and the aircraft responses with a low frequency band-pass filter was developed. The procedure, as previously described, was really nothing more than a fast and simple method of performing harmonic analysis of the traces and required that the data be recorded on magnetic tape. The technique was a valuable one, and it was felt by the authors that it could be utilized to advantage in all forms of steady state dynamic flight testing where telemetering and magnetic recording of data is performed.

The use of telemetering equipment in a flight test program of this sort requires more complicated instrumentation than the simple SFIM

recorder utilized in Ref. 1, in that a ground station and its associated equipment is required. The actual instrumentation in the aircraft is little complicated by the substitution of the telemeter transmitter for the in-flight recorder. The utility derived from having magnetic tape recordings when the telemeter scheme is used is enormous, and it is felt that the advantages of this method outweigh the complications presented by the extra instrumentation required. The filter technique of course would be impossible without tape-recorded data, but in addition tape records of this sort may be expanded to any desired time scale making phase angle measurements easier and more accurate. It is also possible to amplify small responses to distinguishable values, but care must be taken not to exceed the accuracy of the record. The telemetering scheme utilized here was accurate to 1% of full scale and thus small responses could be expected to have a much greater percentage error than large ones. It was therefore desirable during this investigation to obtain responses which were as large as possible without exceeding the range of linearity of the equations of motion. This was accomplished by varying the forcing function amplitudes over the frequency range to give desirable responses. In general, large control deflections were required at high frequencies and small ones at and below the dutch roll frequency.

The method used in this investigation to determine stability derivatives from frequency response was basically sound. As mentioned

previously, considerable difficulty was encountered in the determination of the cross derivatives, and it was felt that accurate determination of these would require much more accurate frequency response data than could be obtained with the simple instrumentation utilized here. The accurate determination of phase angles from data obtained using the forced sinusoidal oscillation technique is difficult indeed, and phase angle errors can have a large effect in the equations for the solution of the stability derivatives, especially when the coefficients of these equations involve sines of angles near 0^{o} or 180^{o} or cosines of angles near 90^{o} or 270^{o}. The technique developed here, which involved fairing a smooth curve through the experimental points and taking data for the computation of the derivatives from the smooth curve, eliminated some of this difficulty, although it was felt that the method of averages could probably eliminate most of this random error even if individual data points were used.

The equations derived from the rudder data were, as previously mentioned, ill-conditioned for solution, and this fact required determination of some of the derivatives from the aileron data before the rudder equations could be used. In theory, it is possible to determine all the derivatives, except of course the aileron control derivatives, from rudder data alone. While this was not possible for the Navion aircraft at the condition investigated, it was felt that for other aircraft or other flight conditions the difficulties encountered here might not be present.

It became apparent to the authors that a need exists for extensive study of the determination lateral stability derivatives from frequency response data, especially as concerns ill-conditioned equations and possible methods for their solution. While it finally proved possible to obtain fairly accurate derivatives in this investigation, certain deviations from the basic method were required. The methods applied here were peculiar to this particular aircraft and flight condition and might very well prove unsuccessful for other aircraft or flight conditions. The best procedure to follow in the extraction of stability derivatives from frequency response data is, at the present time, a function of the type and accuracy of the data, although the authors feel that with time a standardized procedure for eliminating difficulties could be developed.

The use of the method of averages for eliminating random error instead of the method of least squares, as outlined in Ref. 4, proved quite satisfactory and had the added advantage of reducing the computation time considerably. When using this method care must be taken when grouping the points for averaging. If automatic computing facilities are available and large amounts of data require reduction, the method of least squares would probably prove more satisfactory and less subject to error.

It was difficult in this analysis to acquire a feel for the accuracy of many of the individual derivatives. As previously stated, the nature of the equations and the fact that small differences of large quantities

were involved in the solution for C_{y_β}, C_{l_r}, and C_{n_p} made the accuracy of these derivatives questionable. In the solution for $C_{y_{\delta_r}}$, $C_{l_{\delta_r}}$, and $C_{n_{\delta_a}}$ the controlling terms involved C_{y_β}, C_{l_r}, and C_{n_p} respectively, and thus these control derivatives were also of doubtful accuracy. Lateral acceleration data would have eliminated this difficulty in the case of the side force derivatives, but was not obtained here. In the determination of the other derivatives, however, the potential degree of accuracy was not evident from the equations.

A solution of the characteristic equation using the experimentally derived derivatives resulted in a period of 2.38 seconds and a time to half amplitude of 1.69 seconds for the dutch roll mode. Transient data obtained for the same aircraft at the same flight conditions indicated a period of 2.40 seconds and a time to half amplitude of 1.70 seconds. In view of this close agreement, it was concluded that C_{n_β}, which primarily determines the period of the dutch roll mode, and C_{n_r}, the primary damping derivative, were accurately determined.

A comparison of the frequency responses derived from the experimentally determined derivatives and the experimental points indicated certain regions of discrepancy. In Fig. 19 the calculated amplitude response in roll to aileron oscillations was noticeably low at and above the dutch roll frequency, and the calculated phase angle was slightly high in the same region. An analysis of the transfer function contained in Table V indicated that an increase in the coefficient of the first power

term in the numerator would remedy this condition. The most obvious means of accomplishing this was an increase in the value of $C_{l_{\delta_a}}$. An increase in this derivative would also increase the constant term in the numerator of the yaw transfer function and thus increase the amplitude response at low frequencies. Fig. 20 shows the need for this correction. While a detailed analysis of the effect of increasing $C_{l_{\delta_a}}$ was not performed, these considerations led to the conclusion that the value determined for $C_{l_{\delta_a}}$ was low, and a comparison with the results of Ref. 5 indicated this to be the case.

In Fig. 22 the calculated amplitude response in roll to rudder oscillations is substantially less than the experimental response at low frequencies and the phase angle is consistently larger for all frequencies. An analysis of the transfer function for this response indicated that an increase in $C_{n_{\delta_r}}$ would tend to correct both these discrepancies. In addition, the calculated low frequency amplitude response and high frequency phase response for sideslip, as shown in Fig. 24, would also be altered favorably by a larger $C_{n_{\delta_r}}$. A comparison with the results of Ref. 5 indicated that the value determined here for $C_{n_{\delta_r}}$ was too low.

Since the match between the calculated and actual responses was generally good with the exception of the cases mentioned above, it was felt that the determination of those derivatives with the greatest effect on the frequency response, i.e., C_{l_β}, C_{n_β}, C_{l_p}, and C_{n_r}, was

good. While detailed curve fitting of individual responses by altering individual derivatives was not considered within the scope of this investigation, such a technique for correcting derivatives might warrant further study.

CONCLUSIONS AND RECOMMENDATIONS

The method utilized in this investigation to determine the lateral frequency response of an airplane proved entirely feasible and could undoubtedly be applied to many current production aircraft. The method, however, had the disadvantage of requiring more flight time than currently popular transient response methods, and thus would not be practical for missile testing.

Accurate determination of frequency response previously required an elaborate system for the generation of an exact sinusoidal forcing function or time consuming harmonic analysis of the data. The filtering technique developed here eliminated these difficulties, and could have wide application in this type of flight testing.

The method utilized here for the determination of stability derivatives from frequency response data proved accurate for those derivatives with significant effect on the frequency response. It was, however, impossible to determine C_{n_p}, C_{l_r}, $C_{n_{\delta_a}}$, and $C_{l_{\delta_r}}$ with a high degree of accuracy. Better results could have been realized in the determination of C_{y_β} and $C_{y_{\delta_r}}$ if lateral acceleration data had been obtained, and it is recommended that such measurements be made in future tests. It is further recommended that a study be made to develop a systematic method for eliminating the difficulties encountered here with ill-conditioned equations.

REFERENCES

1. Ekas, C. P., Prichard, R. P., and Townsend, M. W.: The Longitudinal Frequency Response of a Navion Airplane from Steady State Dynamic Testing Utilizing Simplified Instrumentation, Princeton University Aeronautical Engineering Report No. 348, 1956.

2. Smith, R. P. and Vogt, L. F.: Determination of the Static Lateral and Directional Derivatives of an Airplane by Steady State Flight Testing, Princeton University Aeronautical Engineering Report No. 302, 1954.

3. Donegan, James J., Robinson, Samuel W., and Gates, Ordway B.: Determination of Lateral-Stability Derivatives and Transfer-Function Coefficients from Frequency-Response Data for Lateral Motions, NACA Report 1225, 1955.

4. Scarborough, J. B.: Numerical Mathematical Analysis, Third Edition, Johns Hopkins Press, Baltimore, Md., 1955.

5. Adams, R. D., Cooper, C. R., and Dedman, T. F.: An Investigation of the Feasibility of Obtaining Lateral Stability Derivatives for a Linear Aircraft by Matching Analog Computer Transient Responses to Flight Test Data, Princeton University Aeronautical Engineering Report No. 384, 1957.

6. Perkins, Courtland D., and Hage, R. E.: Airplane Performance Stability and Control, John Wiley and Sons, Inc., New York, 1949.

7. Hall, Ian A. M., and Reynolds, Philip A.: An Investigation of a Simple Technique for Obtaining Lateral Stability Parameters by Dynamic Flight Tests, Princeton University Aeronautical Engineering Report No. 309, 1955.

BIBLIOGRAPHY

Campbell, C. F., Dynamic Lateral Stability Flight Tests of a B-25J Airplane by Forced Oscillation Method, Cornell Aeronautical Laboratory, Report No. TB-405-F-7, 1947.

Advisory Group for Aeronautical Research and Development Flight Test Manual, Volume II, Stability and Control, Edited by Perkins, Courtland D., Princeton, N. J., 1954.

Advisory Group for Aeronautical Research and Development Flight Test Manual, Volume IV, Instrumentation Systems, Edited by Durbin, Enoch J., Princeton, N. J., 1957.

TABLE I

PHYSICAL CHARACTERISTICS OF NAVION

A.	**WING**	
1.	Total Wing Area, S_w (includes flaps, ailerons and 19.87 $Ft.^2$ covered by the fuselage)	184.337 $Ft.^2$
2.	Span b_w	33.378 Ft.
3.	MAC	68.352 in.
4.	Angle of Incidence	
	Root, i_r	+2°
	Tip, i_t	-1°
5.	Twist	
	Aerodynamic	2° 31'
	Geometric	3°
6.	Airfoil Section	
	Root	NACA 4415R
	Tip	NACA 6410R
7.	Aspect Ratio, AR_w	6.044
8.	Taper Ratio, λ_w	0.5265
9.	Dihedral	7.5°
10.	Root Chord	7.2 Ft.
11.	Tip Chord	3.92 Ft.
A-1.	**AILERON** (one Aileron only) (Beaded skin, Frise Nose Balance, No Trailing Edge Extension)	120°-120° Wheel Throw Fixed bend tab on right aileron.
1.	Area, S_a	2.161 $Ft.^2$
2.	Span, b_a	61.987 in.
3.	Aileron Deflection, δ_a	30° UP, 20° DN.
4.	Boost	None
5.	Trim Tab	Fixed bend tab on right aileron.

B. HORIZONTAL TAIL

1. Total Area (Includes 2.368 Ft.^{2} covered by fuselage)	43.051 Ft.^{2}
2. Span, b_H	13.172 Ft.
3. Airfoil Section	NACA 0012
4. Taper Ratio, λ_t	.67
5. MAC, $\bar{c}_t$	3.34 Ft.
6. Aspect Ratio, AR_t	4.02

B-1. HORIZONTAL STABILIZER

1. Area, S_s	28.953 Ft.^{2}
2. δ_H (with reference to FRP)	-4°

B-2. ELEVATORS (No Trailing Edge Extensions)

Smooth Skin
Flat sided
No trim bungee
Balance spring

1. Total Area, S_e	14.098 Ft.^{2}
2. Span, b_e	73.582 in.
3. Deflection, δ_e	30° UP, 20° DN.
4. Trim Tabs (32" Span, 4-1/2" Chord)	30° UP, 30° DN.
5. Root Chord	1.5 Ft.
6. Tip Chord	1.0 Ft.

C. VERTICAL TAIL

1. Total Area, S_v (Includes 2.577 Ft.^{2} blanketed by fuselage and excluding 1.483 Ft.^{2} of dorsal fin)	12.925 Ft.^{2}
2. Airfoil Section	
Root	NACA 0013.2 Mod.
Tip	NACA 0012-64 "

C-1. VERTICAL STABILIZER

1. Area, S_{V_S} (Includes 0.1427 Ft.^{2} blanketed by fuselage)	6.873 Ft.^{2}
2. α (With reference to fuselage $\mathcal{L}$)	2° Nose left

C-2. RUDDER	Smooth Skin Rigged 3° Rt. to Fin $\mathcal{L}$, Fixed Bend Tab.
1. Area, S_r	6.052 Ft.^{2}
2. Rudder Deflection, δ_r	17° L - 23° R
3. Rudder Pedal Throw	5.75 in.
4. Trim Tab	Fixed Bend Tab

D. PROPELLER	Hartzell
1. Activity Factor, A.F.	100
2. Diameter, d	86"
3. Pitch θ @ .75 R	21° 30'

E. NOSE GEAR	
1. Travel	± 30°
2. Strut Angle (To Vertical)	10°

F. MISCELLANEOUS	
1. Length, overall	27.25 Ft.
2. Tail length, l_{VT}	16.88 Ft.

G. POWER

1. Engine	Continental E-185 Engine 185 HP @ 2300 RPM, 29" Hg M.P. @ Sea Level

TABLE II

EXPERIMENTAL FREQUENCY RESPONSE DATA

TO SINUSOIDAL AILERON OSCILLATIONS

T.A.S. = 129.6 m.p.h.
Density Alt. = 5000 ft.
Gross Wt. = 2870 lbs.

ω	$\left\lvert \frac{\Phi}{\delta a} \right\rvert$	$\Phi_{\Phi\delta a}$	$\left\lvert \frac{\Psi}{\delta a} \right\rvert$	$\Phi_{\Psi\delta a}$	$\left\lvert \frac{\beta}{\delta a} \right\rvert$	$\Phi_{\beta\delta a}$
0.73	3.20	92.0	1.225	- 11.0	.362	173.3
1.14	2.175	76.0	.703	- 7.5	.485	152.2
1.61	1.452	88.2	.637	- 28.9	.566	140.0
1.78	1.322	85.0	.604	- 30.0	.529	145.0
2.23	1.047	95.1	.844	- 54.0	.920	108.1
2.33	1.042	94.0	.881	- 58.0	.806	119.0
2.57	1.197	84.0	.790	-105.0	1.032	72.8
2.59	1.458	88.5	.750	-132.2	1.005	46.0
2.62	1.130	104.4	.820	- 94.0	1.100	85.0
2.79	1.448	90.0	.725	-136.7	.982	46.0
2.97	1.338	83.2	.666	-132.8	.855	28.9
3.27	1.001	69.4	.259	+180.0	.367	8.7
3.79	.899	66.1	.213	172.0	.283	10.0
3.92	.822	65.3	.1608	166.6	.260	356.5
4.63	.681	63.5	.0851	151.0	-	-
5.20	.562	52.0	.0646	131.3	.1265	334.7
5.85	.496	59.0	.0408	125.0	.0775	336.3

TABLE III

EXPERIMENTAL FREQUENCY RESPONSE DATA

TO SINUSOIDAL RUDDER OSCILLATIONS

T.A.S. = 129.6 m.p.h.
Density Alt. = 5000 ft.
Gross Wt. = 2870 lbs.

ω	$\left\lvert\frac{\Phi}{\delta r}\right\rvert$	$\Phi_{\Phi\delta r}$	$\left\lvert\frac{\psi}{\delta r}\right\rvert$	$\Phi_{\psi\delta r}$	$\left\lvert\frac{\beta}{\delta r}\right\rvert$	$\Phi_{\beta\delta r}$
1.05	1.222	100.2	7.41	176.2	1.175	6.1
1.315	1.121	94.5	.904	168.4	1.130	4.4
1.615	1.100	94.6	1.053	171.8	1.175	6.1
1.85	1.106	79.4	1.211	160.0	1.51	348.9
1.87	1.352	82.5	1.341	164.0	1.585	347.9
2.21	1.358	57.1	1.810	141.0	2.135	331.4
2.41	1.465	37.3	2.165	119.9	2.55	308.1
2.48	1.48	54.6	2.13	132.5	2.60	313.9
2.58	1.55	21.6	2.21	106.4	2.63	295.5
2.58	1.51	35.4	2.168	124.0	2.46	308.6
2.69	1.547	+ 5.2	2.218	79.5	2.695	281.4
2.99	1.00	-24.5	1.661	73.2	1.99	246.2
3.71	.452	-51.8	.822	38.9	.980	224.9
4.00	.294	-63.6	.599	29.2	.655	210.3
4.35	.253	-58.7	.493	20.0	.552	217.6
4.68	.181	-66.6	.390	30.9	.390	226.5
4.70	.164	-66.5	.364	41.5	.408	215.7
4.83	.160	-68.0	.338	20.0	-	-
5.34	.104	-77.6	.253	19.6	.274	215.2
5.38	-	-	.2435	22.6	.241	215.8
5.71	.083	-75.5	.216	34.5	.243	208.7
7.21	.0447	-83.5	.127	24.0	.1545	197.5

TABLE IV

INITIAL THEORETICAL AND EXPERIMENTALLY DERIVED

LATERAL STABILITY DERIVATIVES FOR THE NAVION

T.A.S. = 129.6 m.p.h.
Density Alt. = 5000 ft.
Gross Wt. = 2870 lbs.

Derivative	Initial Theoretical	Results of Ref. 5	Final Experimental Results
C_{y_β}	-0.592	-0.592	-0.591
C_{l_r}	+0.102	+0.131	+0.119
C_{l_β}	-0.0814	-0.0595	-0.0513
C_{l_p}	-0.460	-0.430	-0.434
C_{n_r}	-0.0937	-0.0951	-0.0908
C_{n_β}	+0.085	+0.101	+0.0895
C_{n_p}	-0.051	-0.0705	-0.106
$C_{y_{\delta_r}}$	+0.123	+0.144	+0.206
$C_{l_{\delta_a}}$	-0.101	-0.137	-0.108
$C_{l_{\delta_r}}$	+0.0152	+0.0069	+0.0128
$C_{n_{\delta_a}}$	+0.0138	+0.0031	+0.00376
$C_{n_{\delta_r}}$	-0.0625	-0.0774	-0.0673

TABLE V

TRANSFER FUNCTIONS FOR THE NAVION DETERMINED

FROM EXPERIMENTAL FREQUENCY RESPONSE DATA

T.A.S. = 129.6 m.p.h.
Density Alt. = 5000 ft.
Gross Wt. = 2870 lbs.

$$(1)\quad \frac{\beta}{\delta a} = \frac{-.244\,s^2 - 20.041\,s - 2.155}{s^4 + 9.002\,s^3 + 13.568\,s^2 + 57.884\,s - 1.631}$$

$$(2)\quad \frac{\Phi}{\delta a} = \frac{-23.470\,s^2 - 17.235\,s - 136.588}{s^4 + 9.002\,s^3 + 13.568\,s^2 + 57.884\,s - 1.631}$$

$$(3)\quad \frac{\psi}{\delta a} = \frac{.244\,s^3 + 11.939\,s^2 + 3.986\,s - 22.894}{s\left(s^4 + 9.002\,s^3 + 13.568\,s^2 + 57.884\,s - 1.631\right)}$$

$$(4)\quad \frac{\beta}{\delta r} = \frac{.868\,s^3 + 11.969\,s^2 + 41.891\,s - 1.450}{s^4 + 9.002\,s^3 + 13.568\,s^2 + 57.884\,s - 1.631}$$

$$(5)\quad \frac{\Phi}{\delta r} = \frac{2.793\,s^2 - 17.475\,s - 28.370}{s^4 + 9.002\,s^3 + 13.568\,s^2 + 57.884\,s - 1.631}$$

$$(6)\quad \frac{\psi}{\delta r} = \frac{-4.376\,s^3 - 33.769\,s^2 + 38.794\,s - 5.598}{s\left(s^4 + 9.002\,s^3 + 13.568\,s^2 + 57.884\,s - 1.631\right)}$$

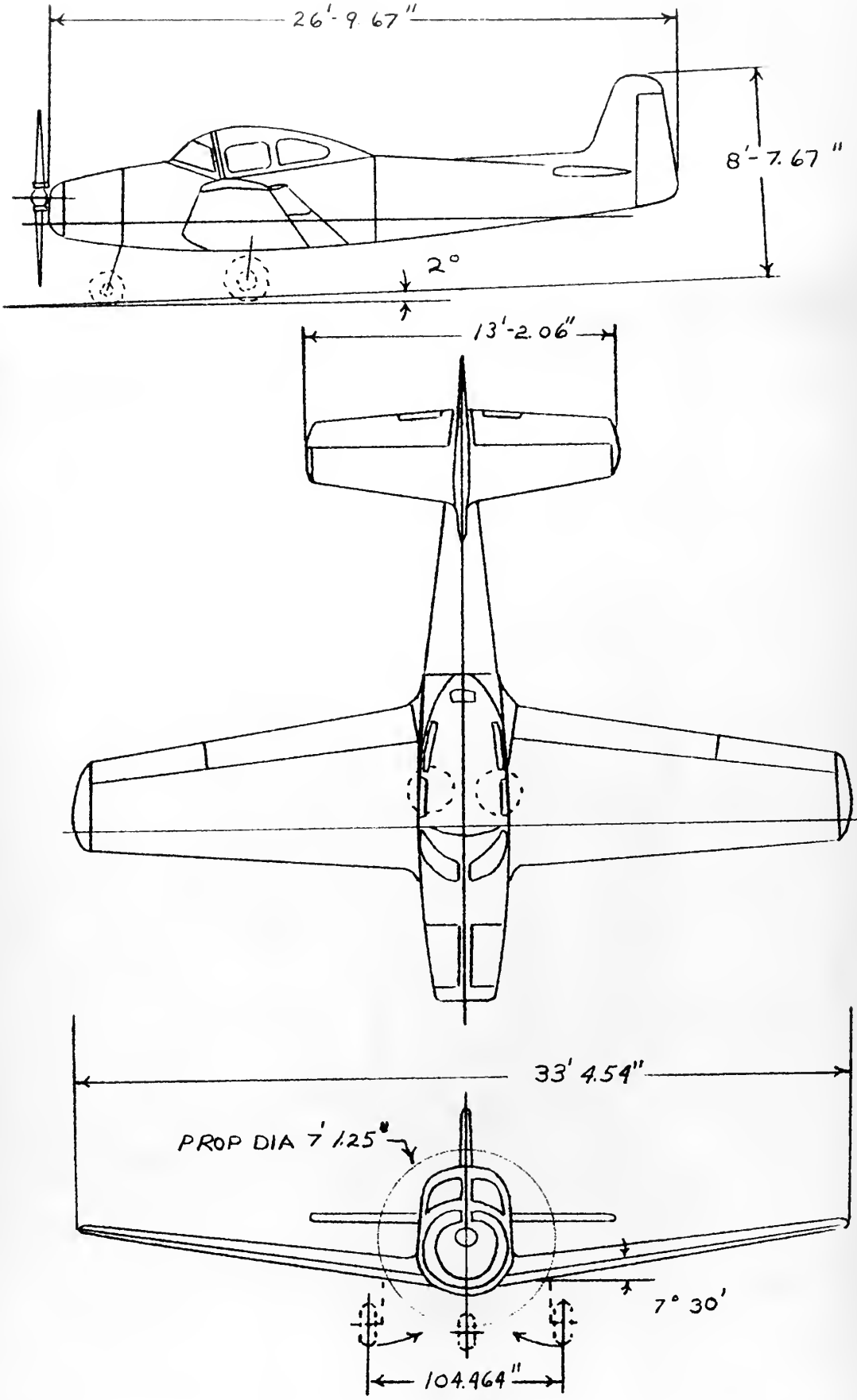

FIG 1

GENERAL THREE-VIEW DRAWING

FIGURE 2 - TEST AIRCRAFT

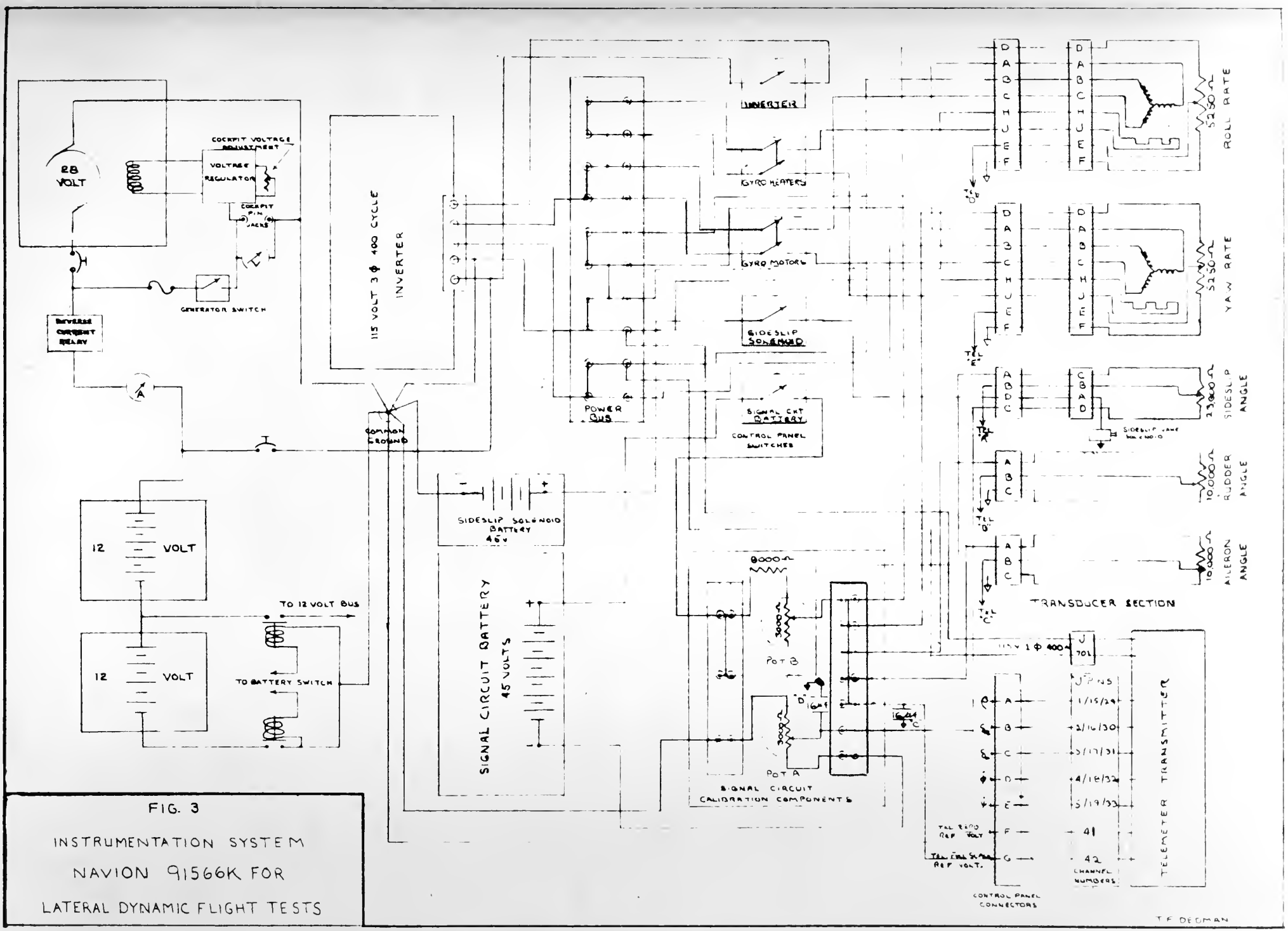

FIG. 3

INSTRUMENTATION SYSTEM

NAVION 91566K FOR

LATERAL DYNAMIC FLIGHT TESTS

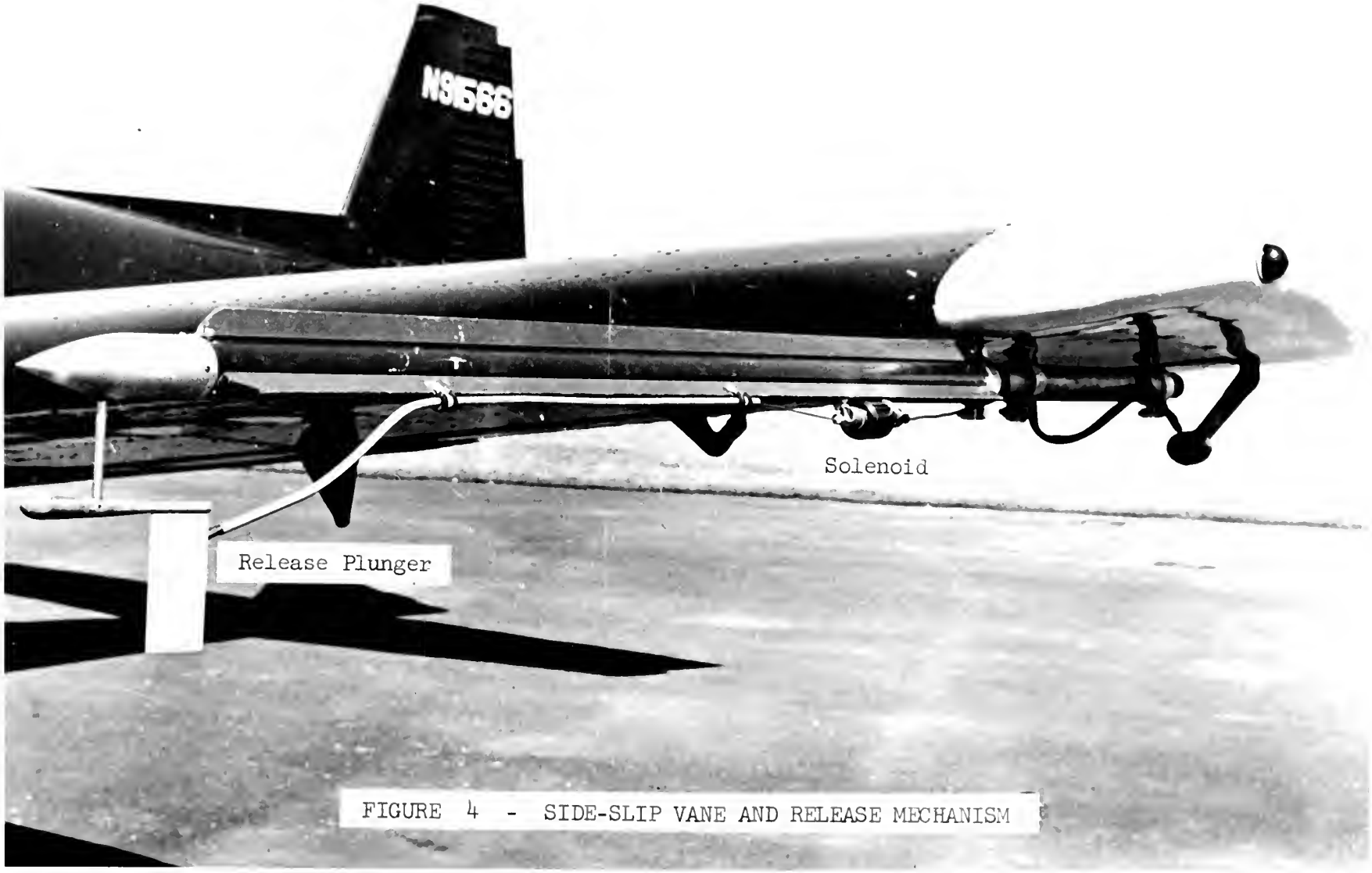

FIGURE 4 - SIDE-SLIP VANE AND RELEASE MECHANISM

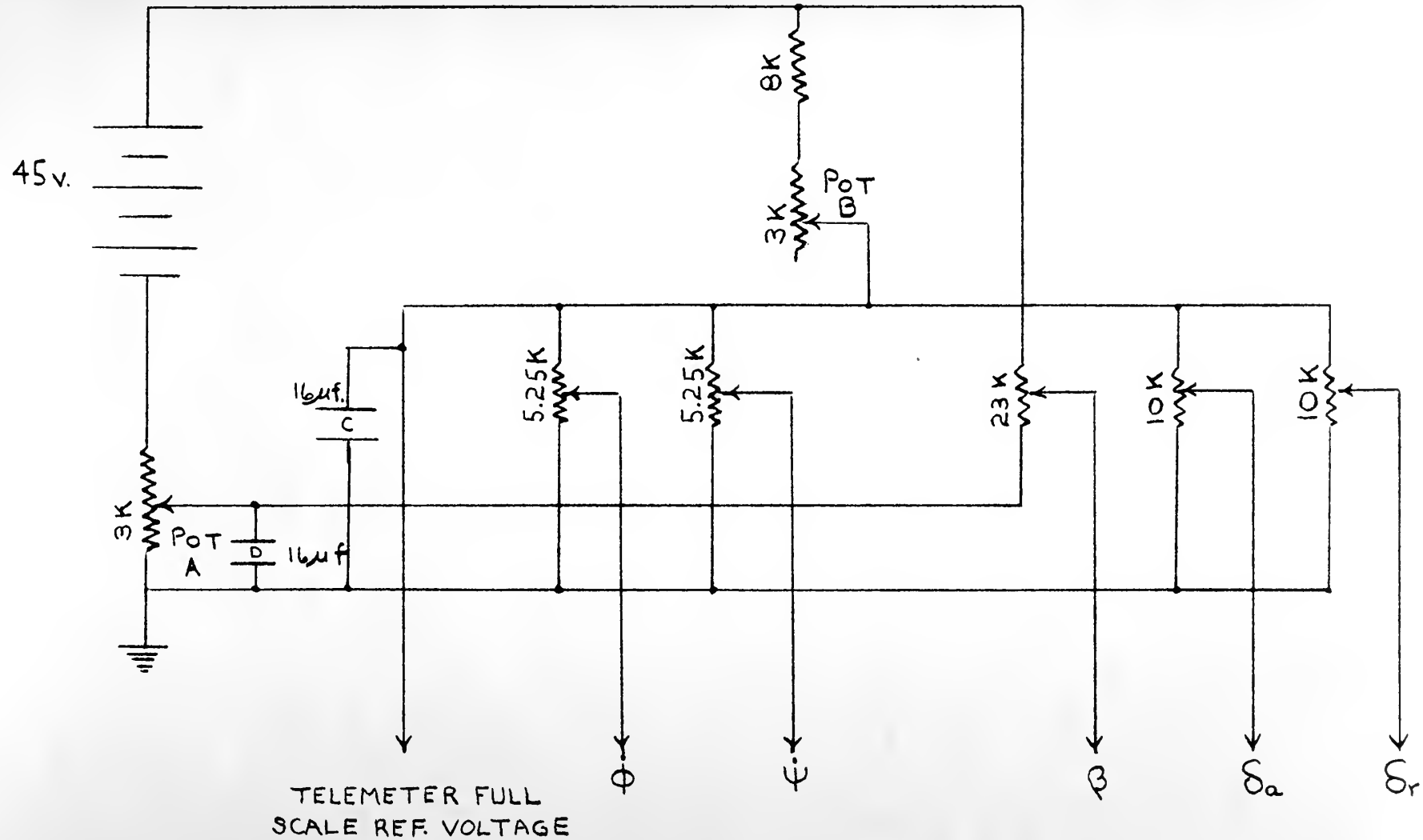

FIG 5

SCHEMATIC OF AIRCRAFT
INSTRUMENTATION CIRCUIT

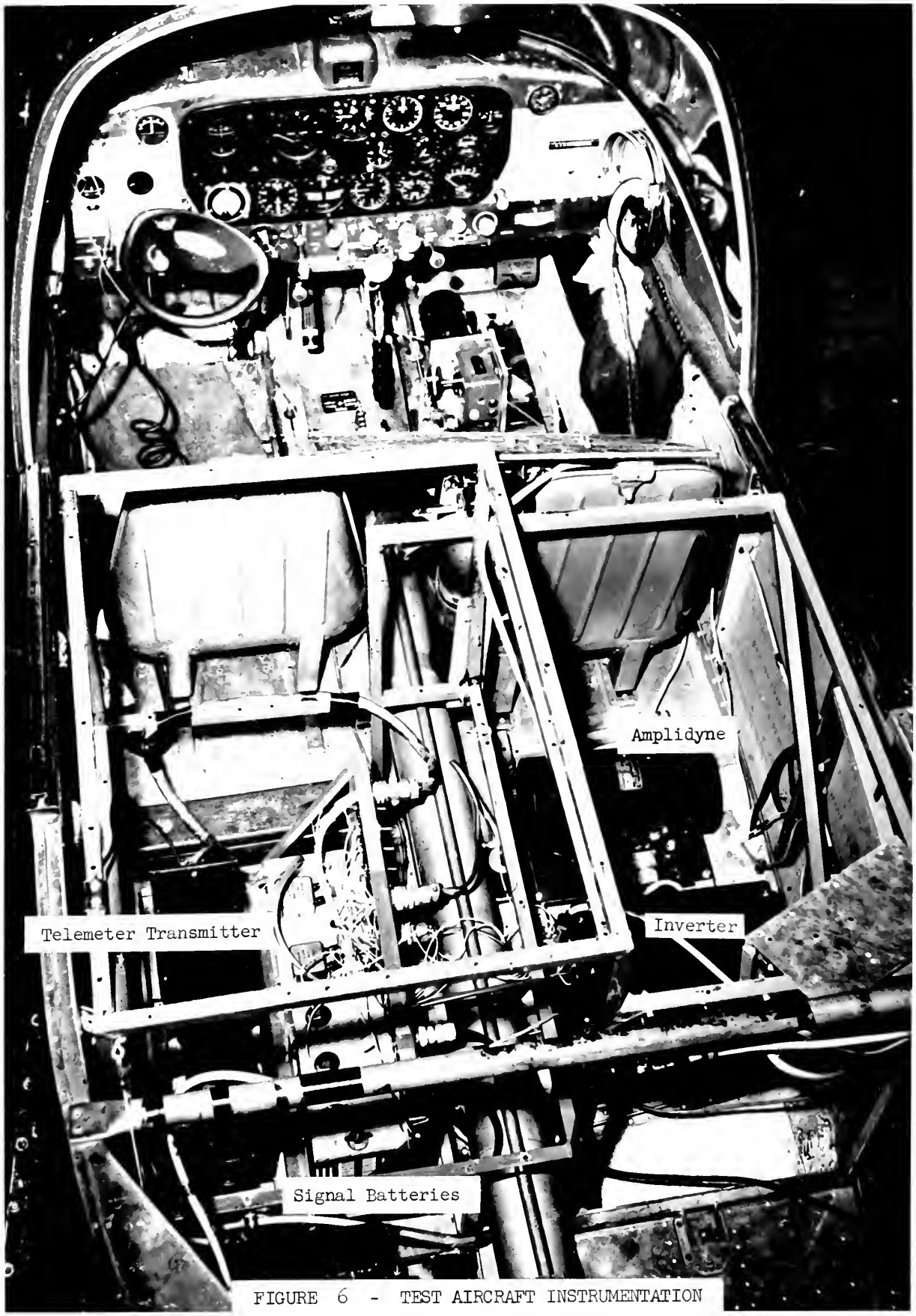

FIGURE 6 - TEST AIRCRAFT INSTRUMENTATION

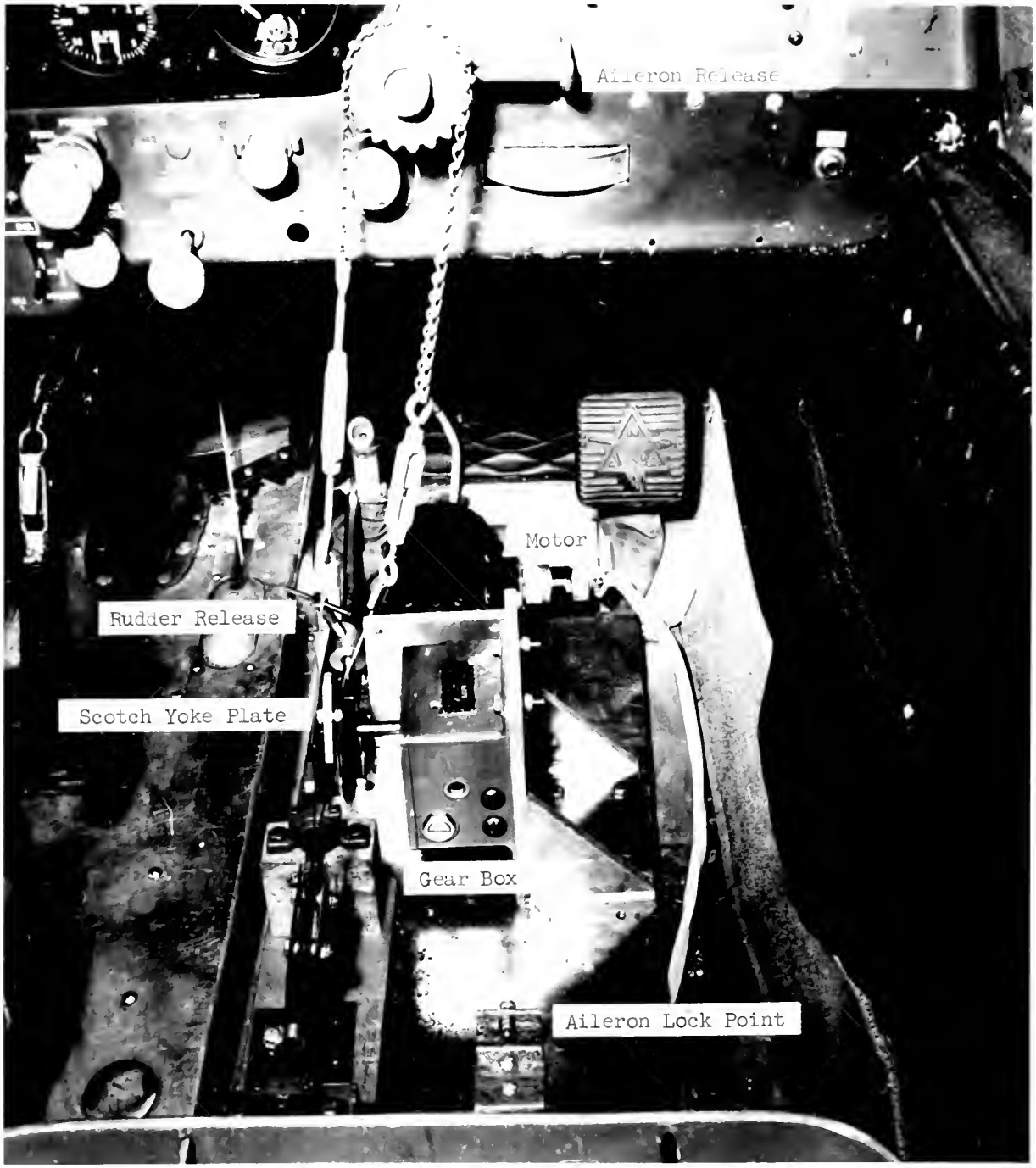

FIGURE 7 - MECHANISM FOR THE SINUSOIDAL OSCILLATION OF AILERONS OR RUDDER WITH PROVISIONS FOR THE LOCKING OF THE UNDRIVEN CONTROL

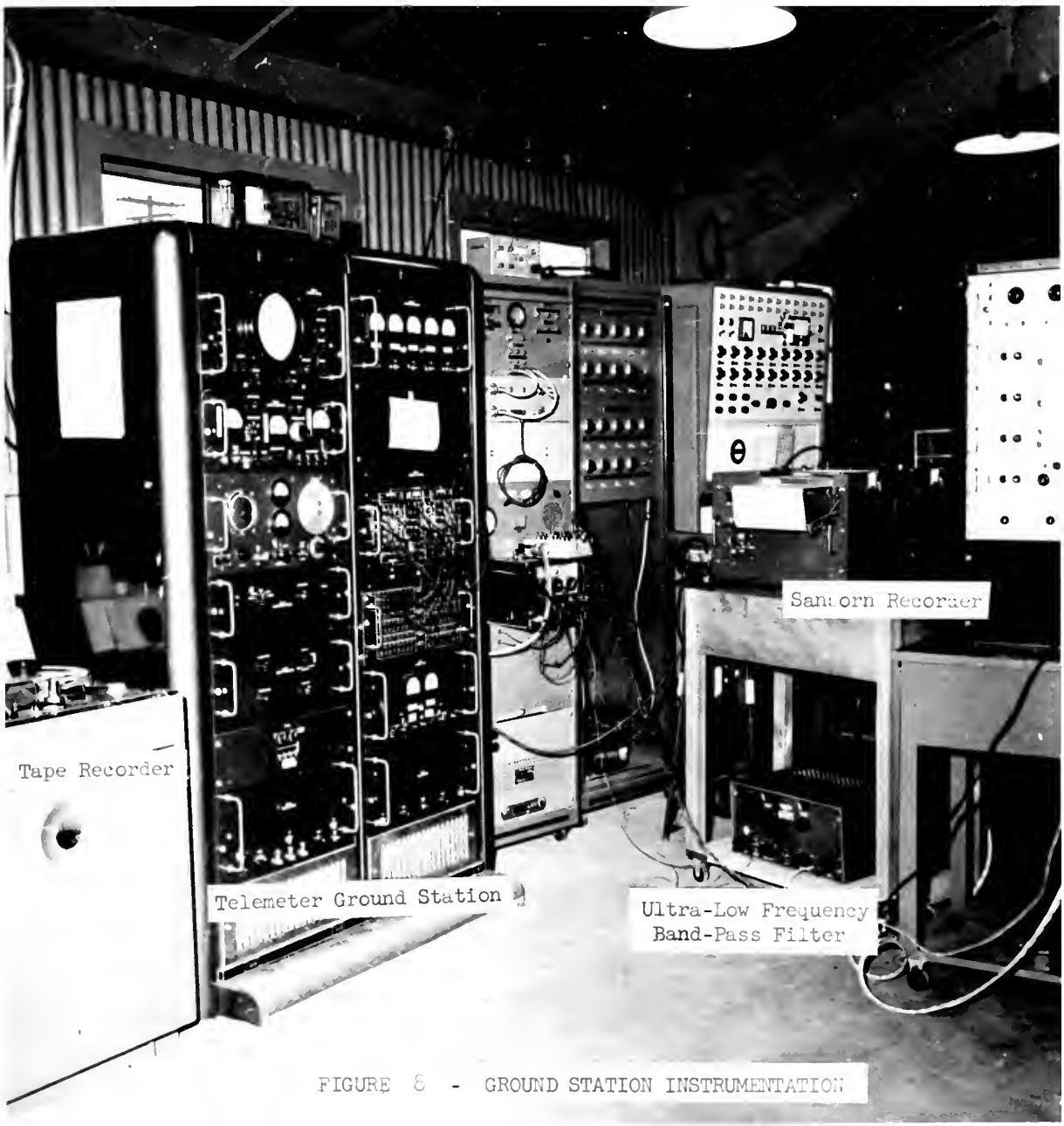

FIGURE 8 - GROUND STATION INSTRUMENTATION

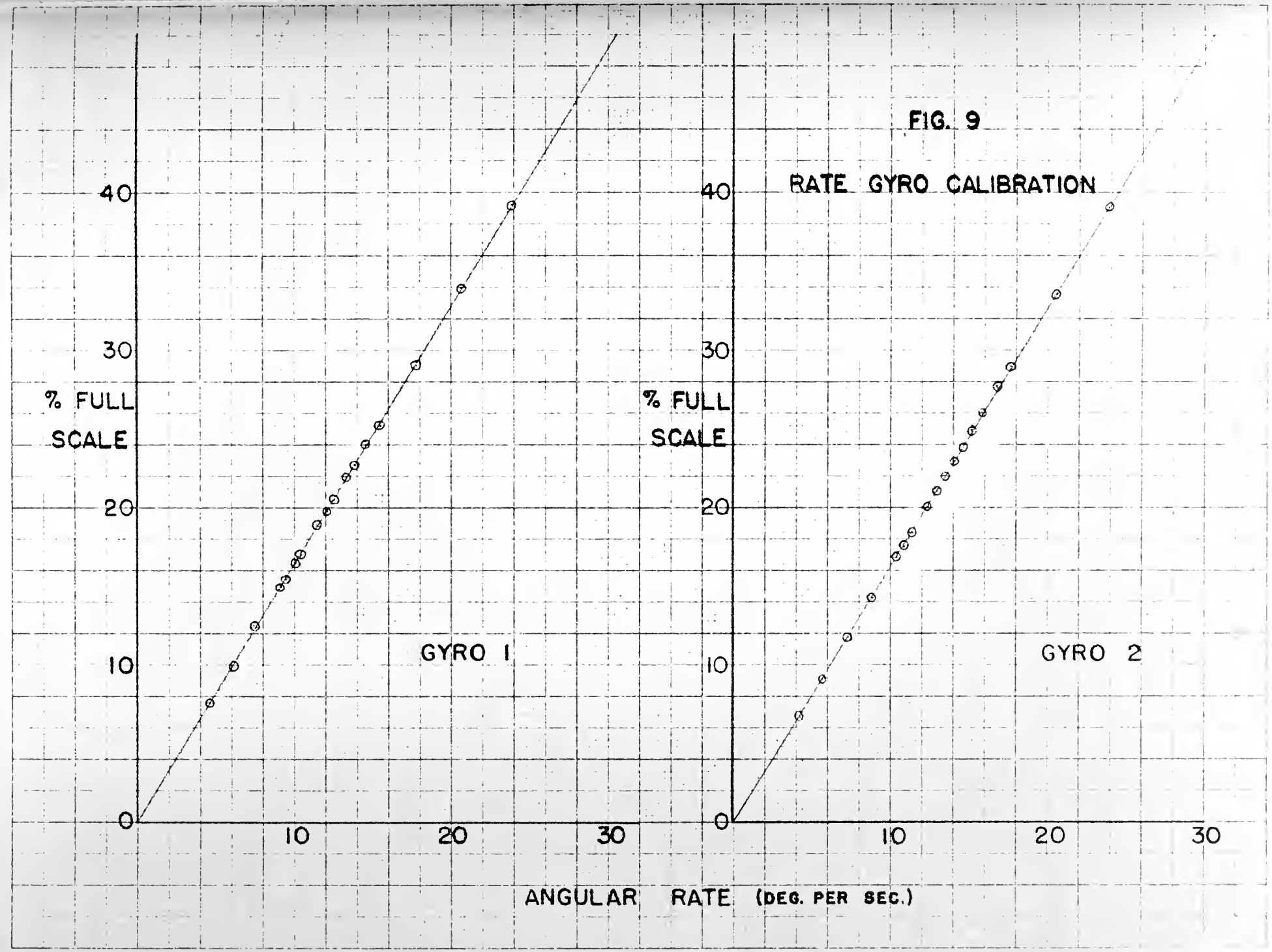
FIG. 9
RATE GYRO CALIBRATION
40
30
20
10
0
% FULL SCALE
GYRO 1
GYRO 2
10
20
30
ANGULAR RATE (DEG. PER SEC.)

FIG. 10

SIDESLIP VANE CALIBRATION

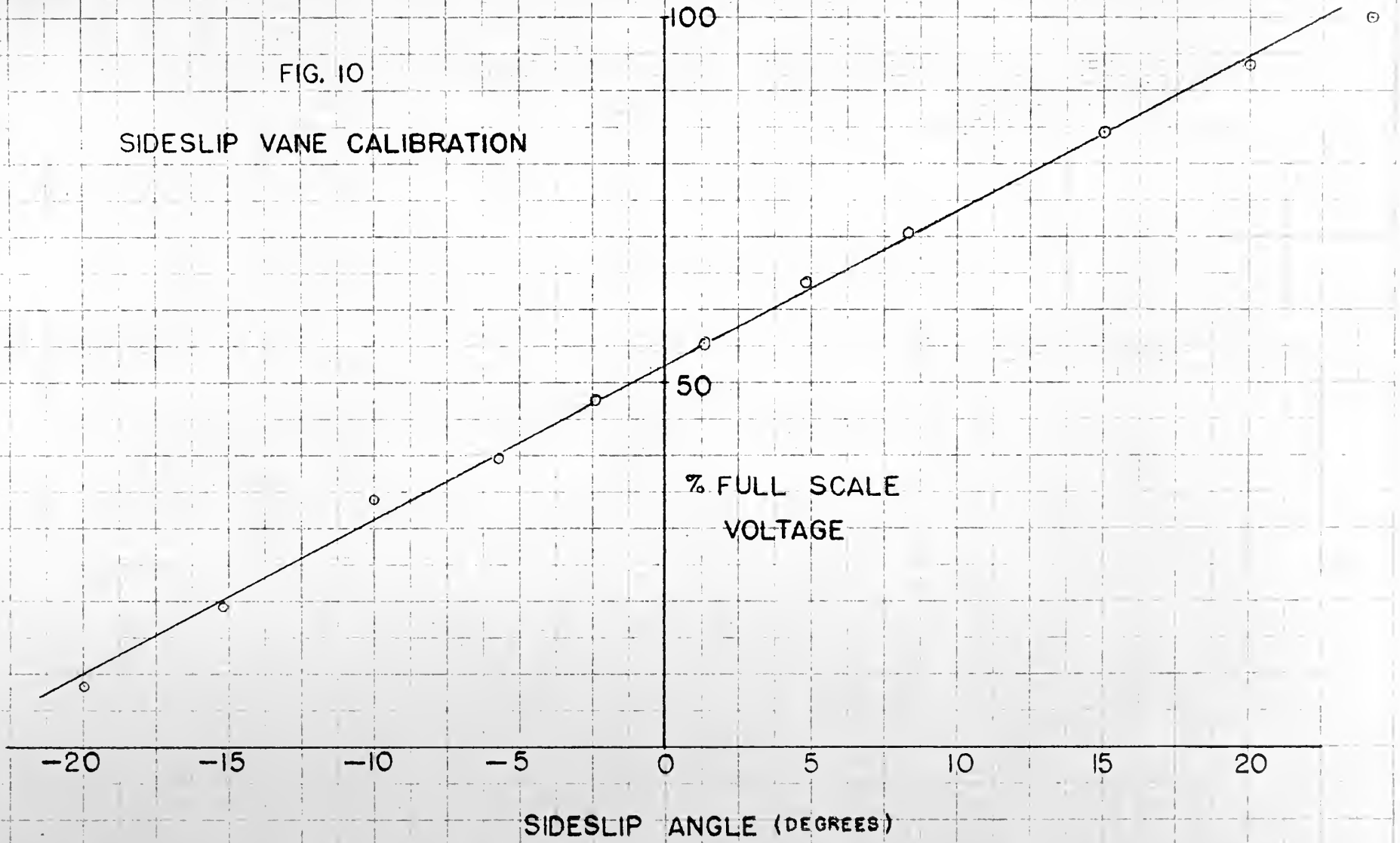

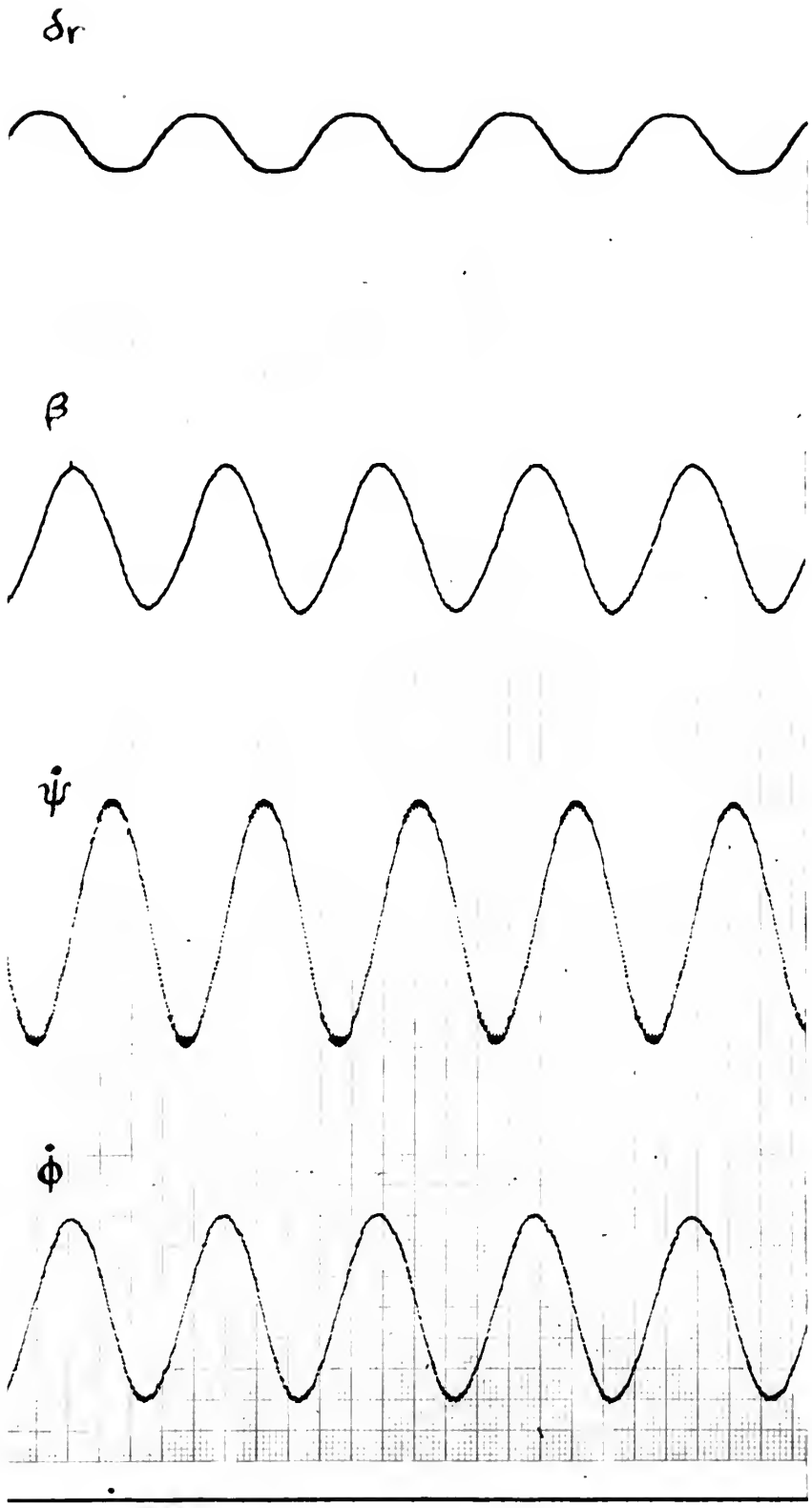

FIGURE 11 - SAMPLES OF RAW DATA

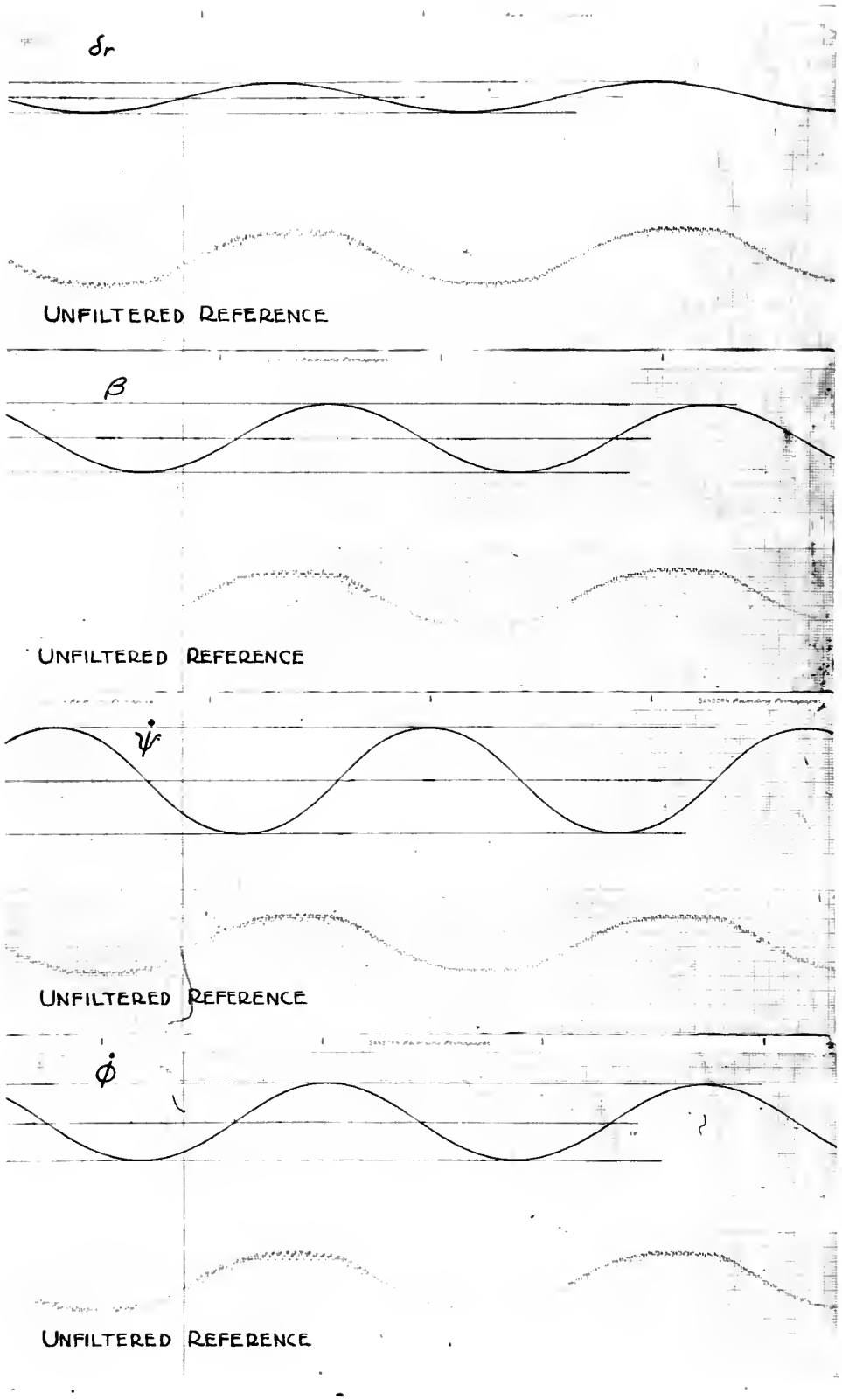

FIGURE 12 - SAMPLES OF FILTERED DATA

FREQUENCY RESPONSE TO AILERON OSCILLATIONS
(ROLL)

FIG. 13 (a)

$\left|\frac{\phi}{\delta_a}\right|$ VERSUS ω

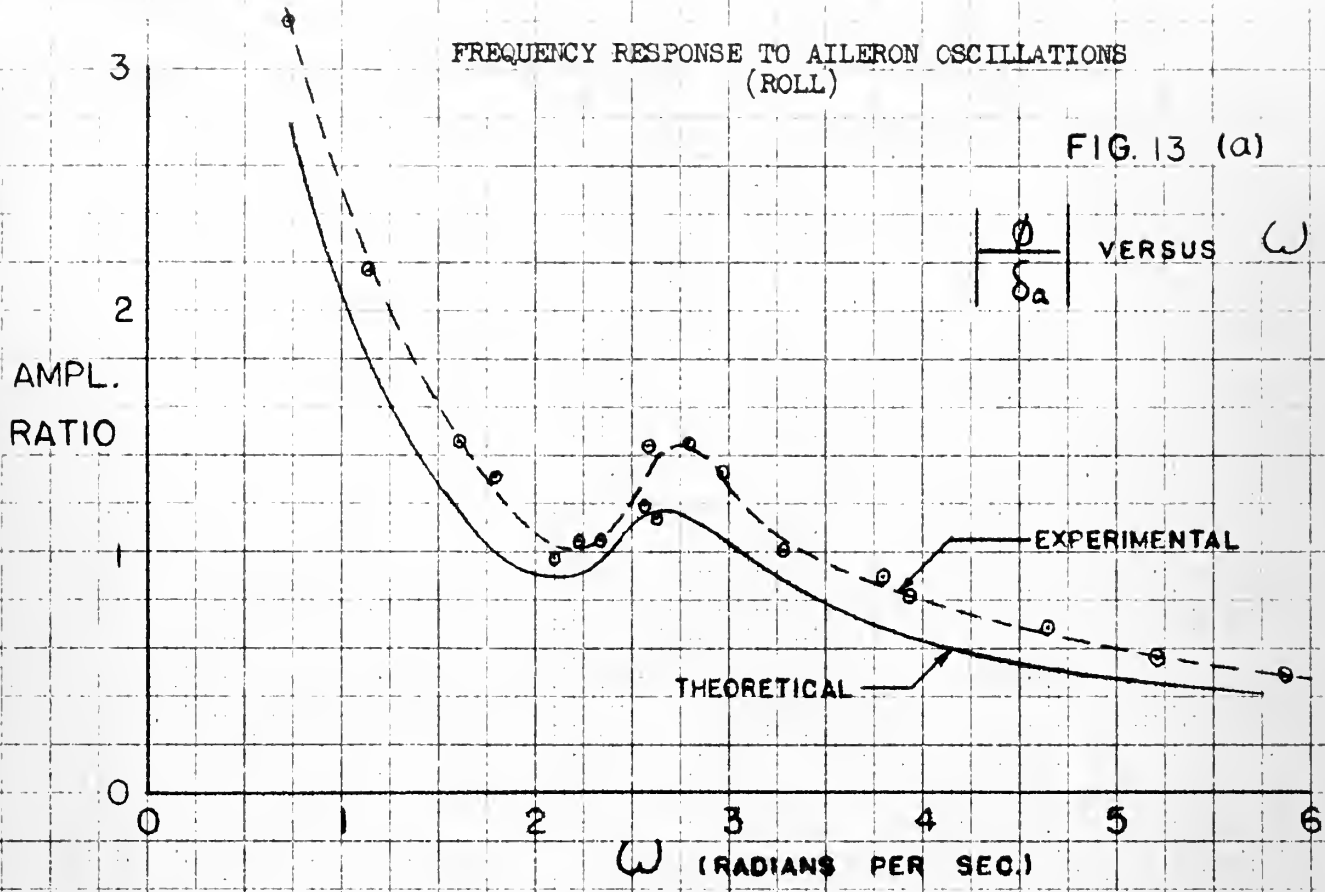

FIG. 13 (b)

$\Phi_{\phi\delta_a}$ VERSUS ω

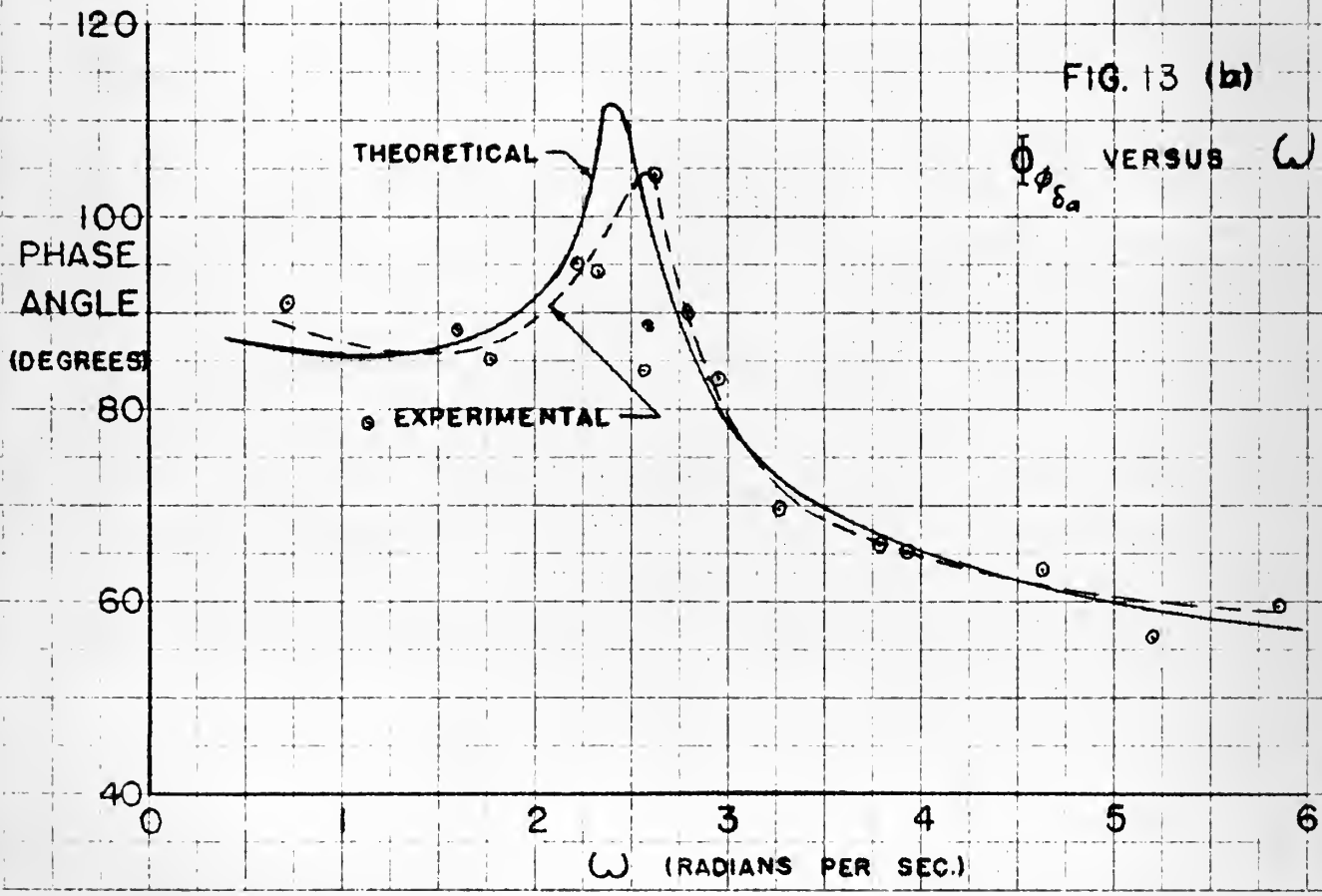

FREQUENCY RESPONSE TO AILERON OSCILLATIONS
(YAW)

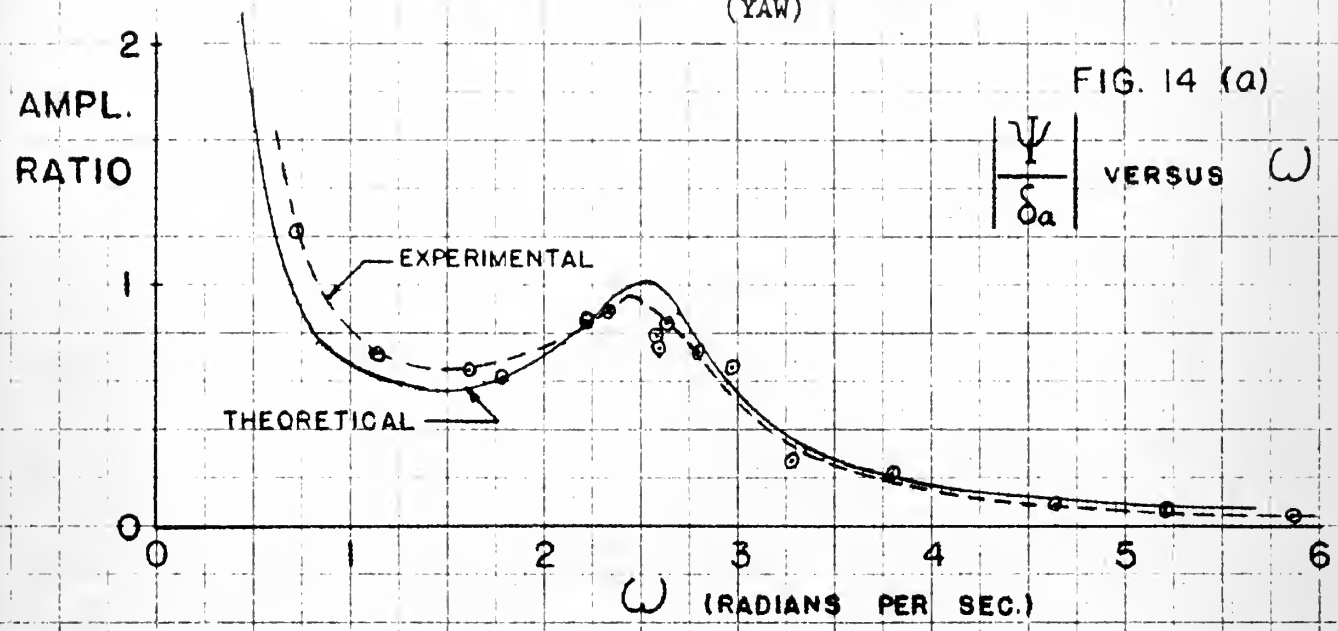

FIG. 14 (a)

$\left|\frac{\Psi}{\delta_a}\right|$ VERSUS ω

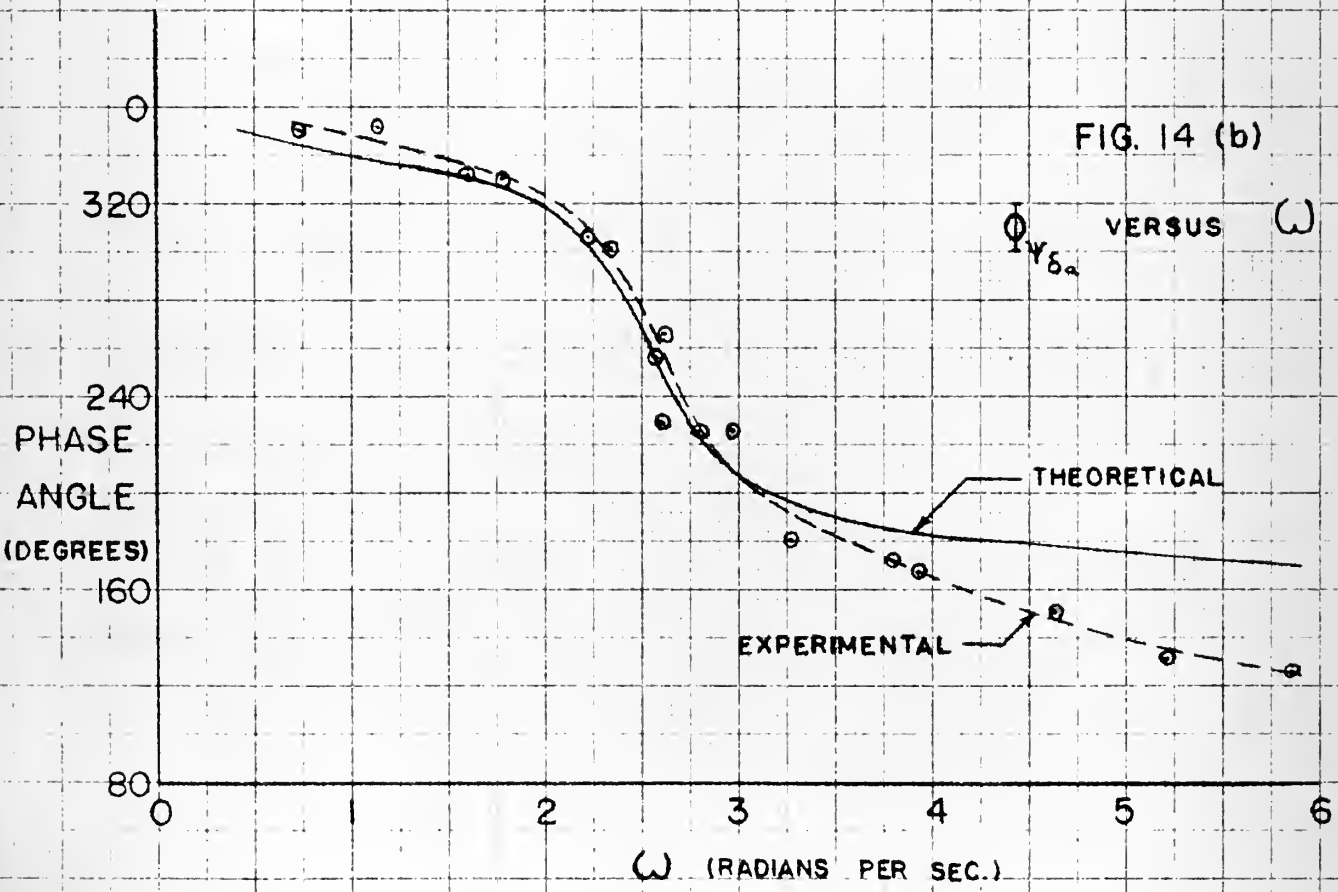

FIG. 14 (b)

$\Phi_{\Psi_{\delta_a}}$ VERSUS ω

FREQUENCY RESPONSE TO AILERON OSCILLATIONS
(SIDESLIP)

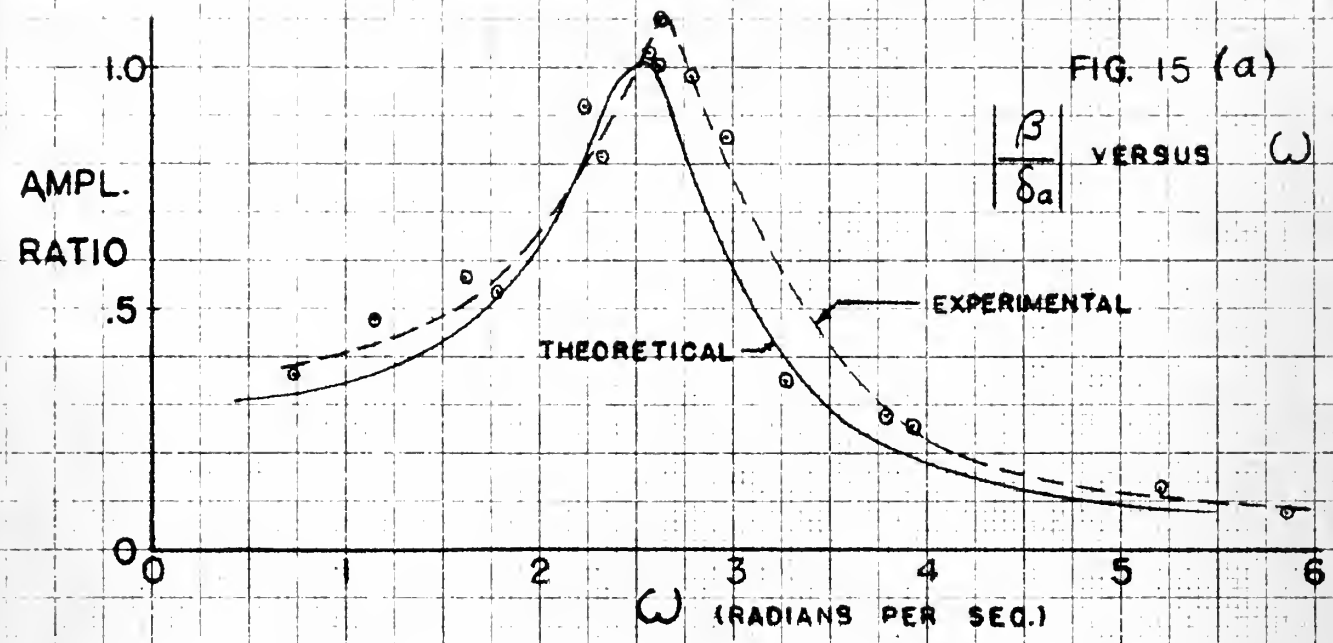

FIG. 15 (a)

$\left|\frac{\beta}{\delta_a}\right|$ VERSUS ω

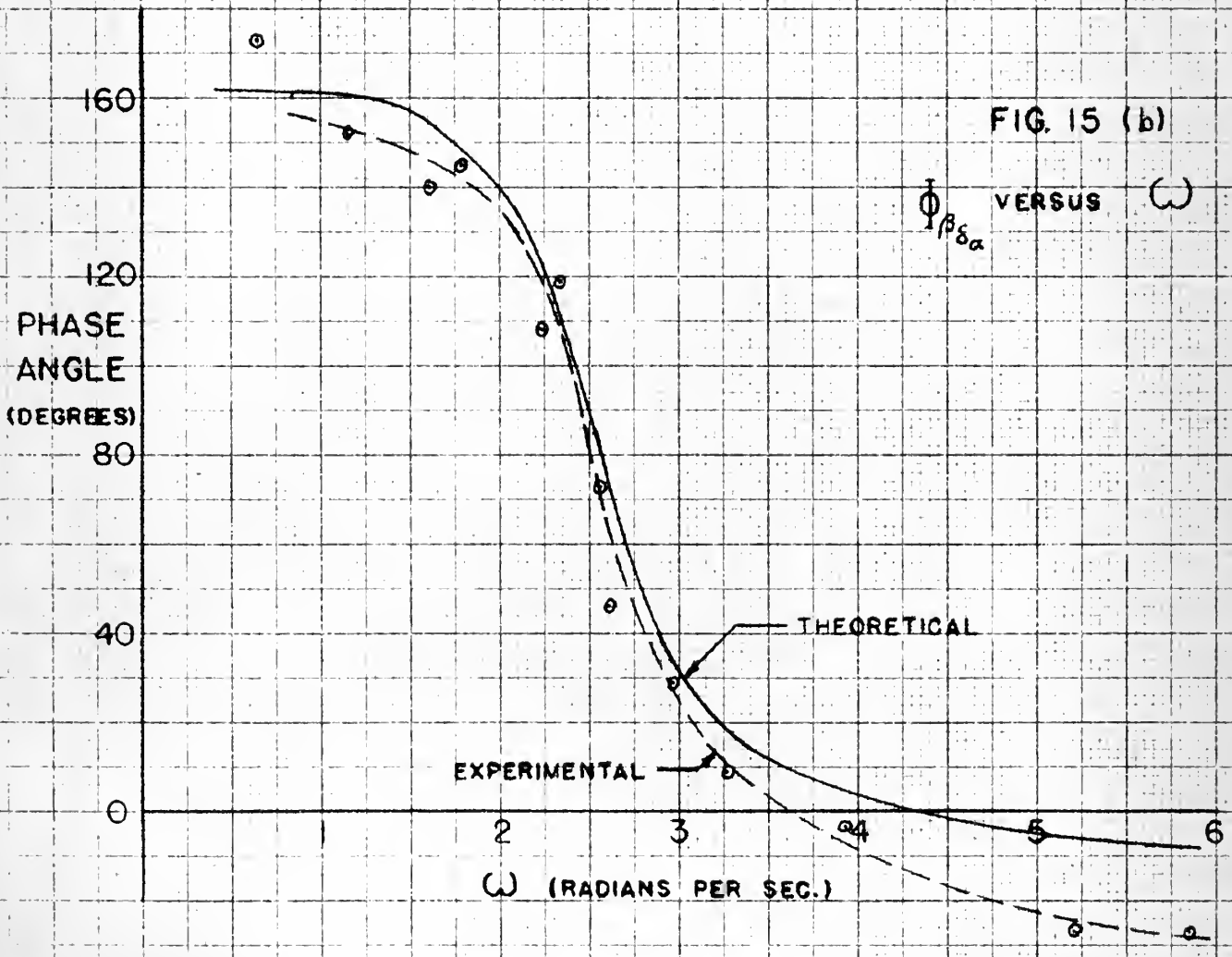

FIG. 15 (b)

$\Phi_{\beta\delta_a}$ VERSUS ω

FREQUENCY RESPONSE TO RUDDER OSCILLATIONS
(ROLL)

FIG. 16 (a)

$\left|\frac{\phi}{\delta_r}\right|$ VERSUS ω

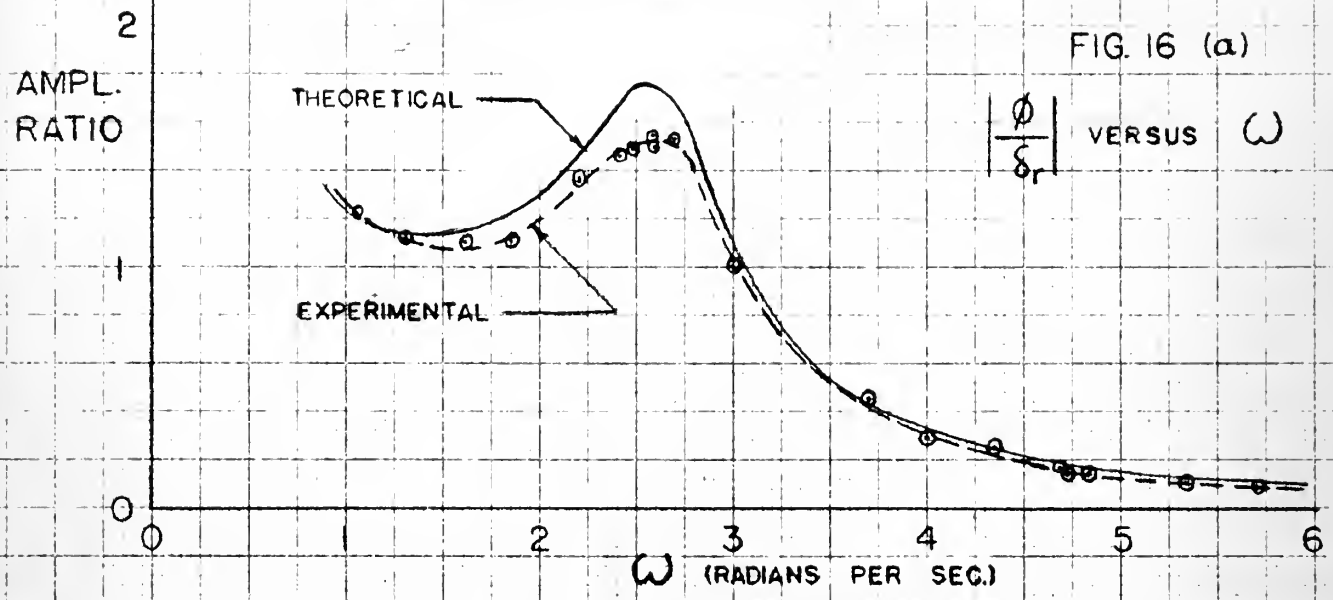

FIG. 16 (b)

$\Phi_{\phi_{\delta_r}}$ VERSUS ω

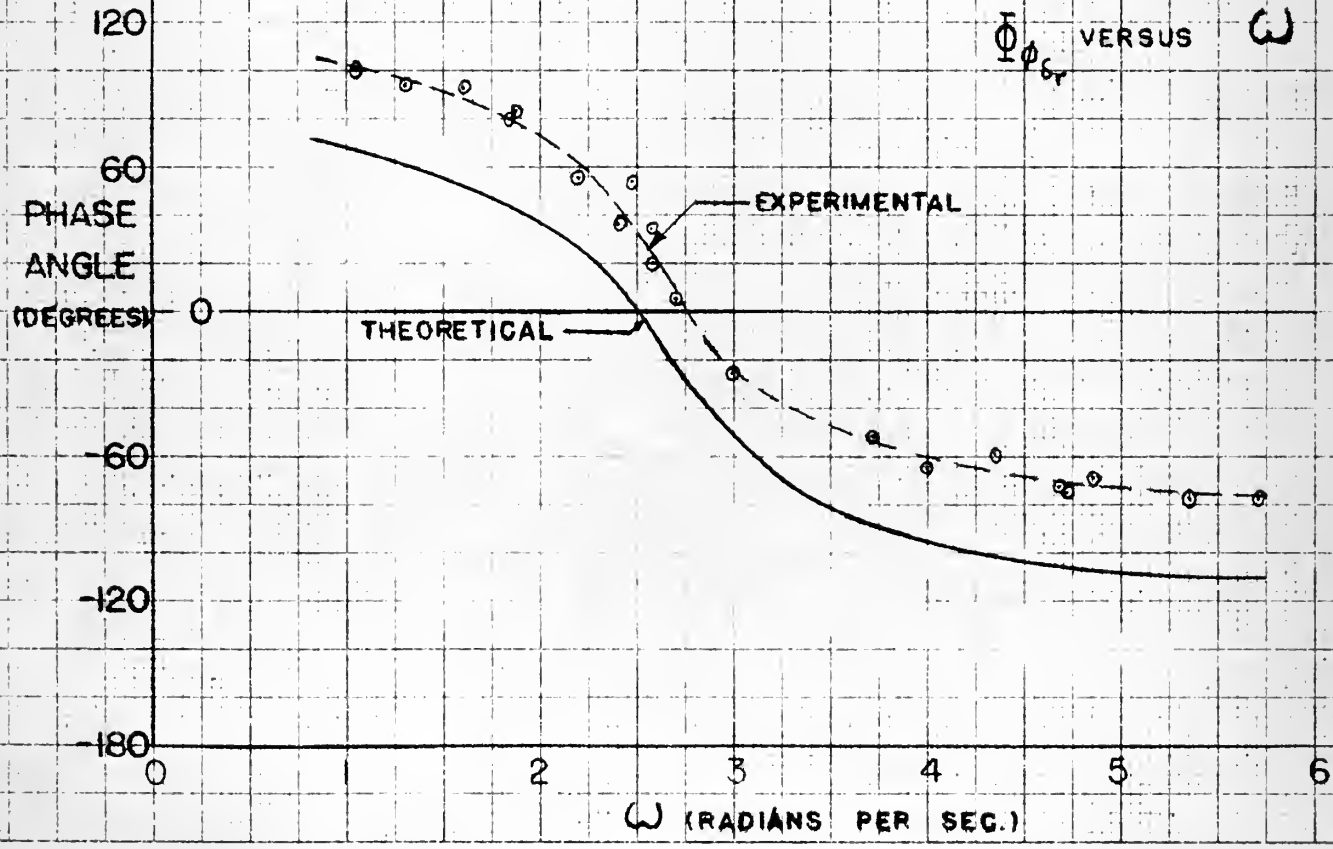

FREQUENCY RESPONSE TO RUDDER OSCILLATIONS
(YAW)

FIG. 17 (a)

$\left|\frac{\Psi}{\delta_r}\right|$ VERSUS ω

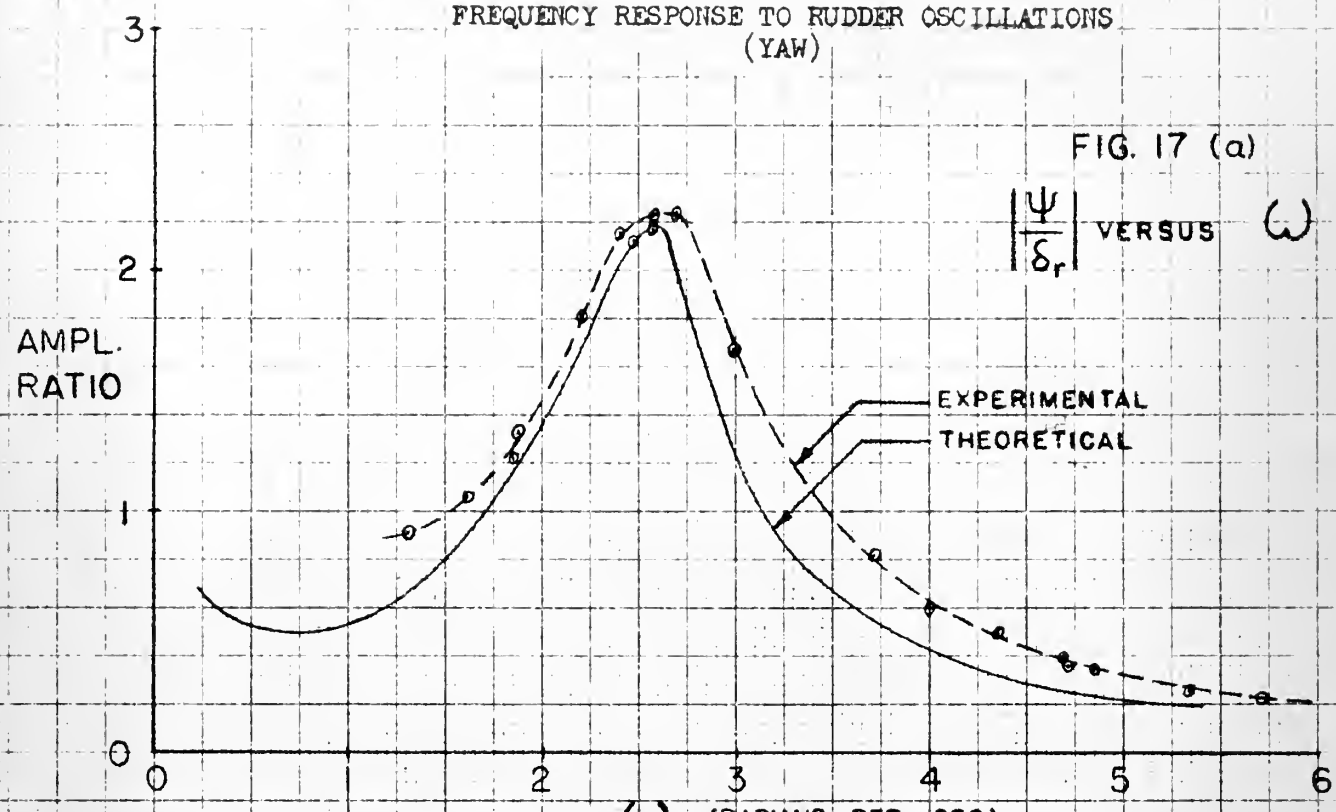

FIG. 17 (b)

$\Phi_{\Psi_{\delta_r}}$ VERSUS ω

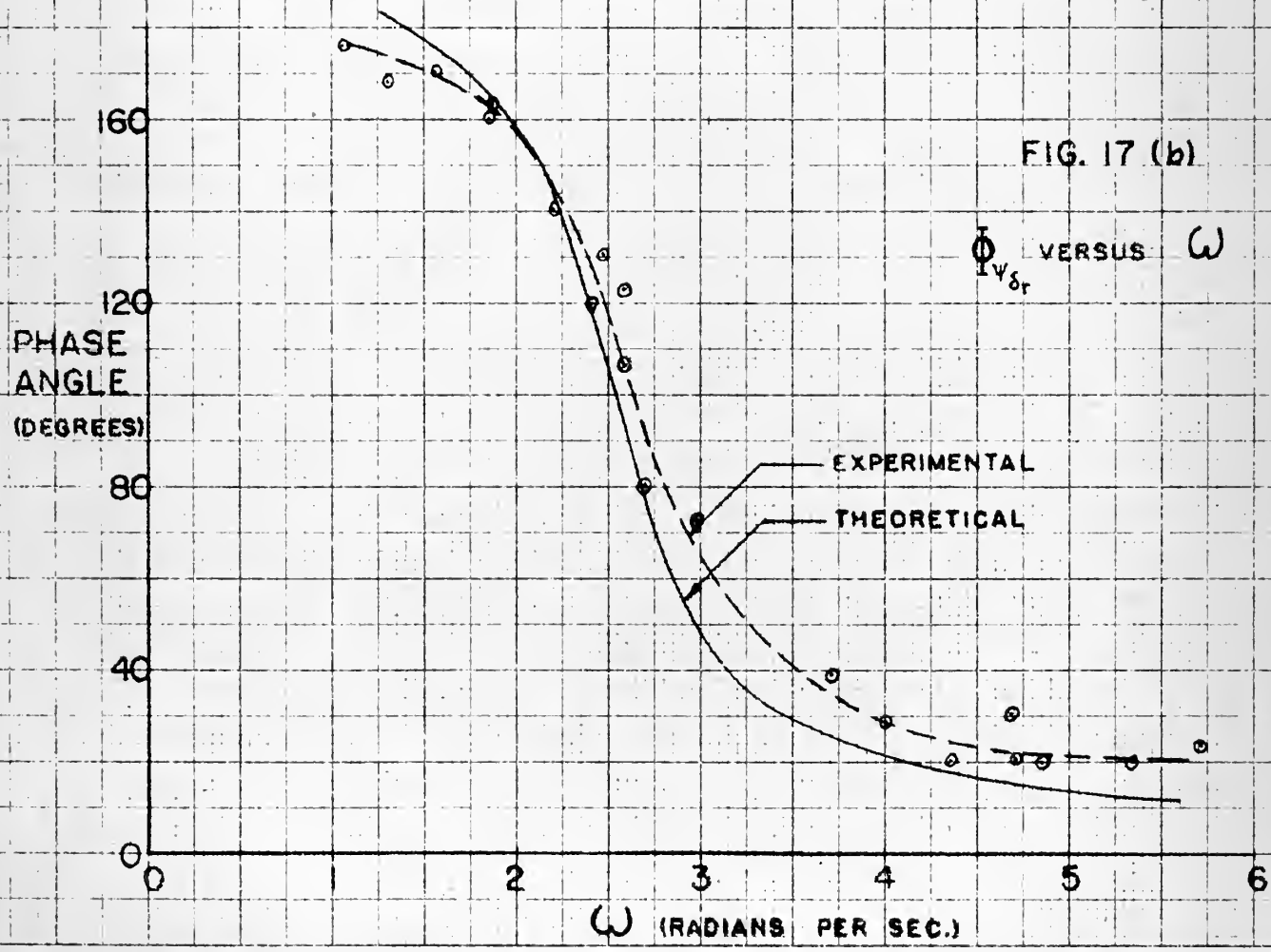

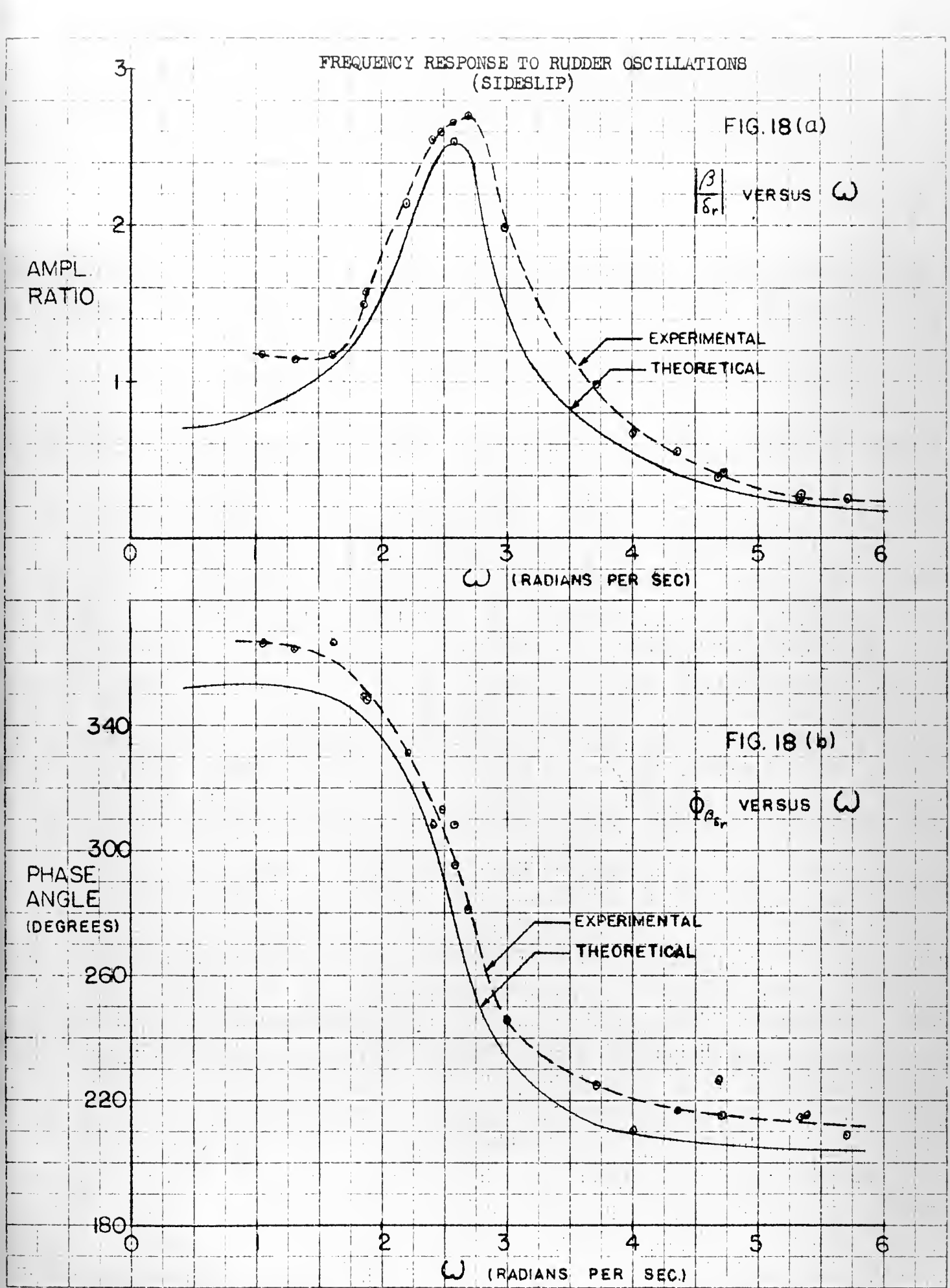
FREQUENCY RESPONSE TO RUDDER OSCILLATIONS
(SIDESLIP)
FIG. 18(a)
$\left|\frac{\beta}{\delta_r}\right|$ VERSUS ω
AMPL. RATIO
3
2
1
0
EXPERIMENTAL
THEORETICAL
1
2
3
4
5
6
ω (RADIANS PER SEC)
FIG. 18 (b)
$\Phi_{\beta_{\delta_r}}$ VERSUS ω
PHASE ANGLE (DEGREES)
340
300
260
220
180
EXPERIMENTAL
THEORETICAL
0
1
2
3
4
5
6
ω (RADIANS PER SEC.)

CALCULATED FREQUENCY RESPONSE IN ROLL
FROM EXPERIMENTALLY DERIVED DERIVATIVES
TO AILERON OSCILLATIONS

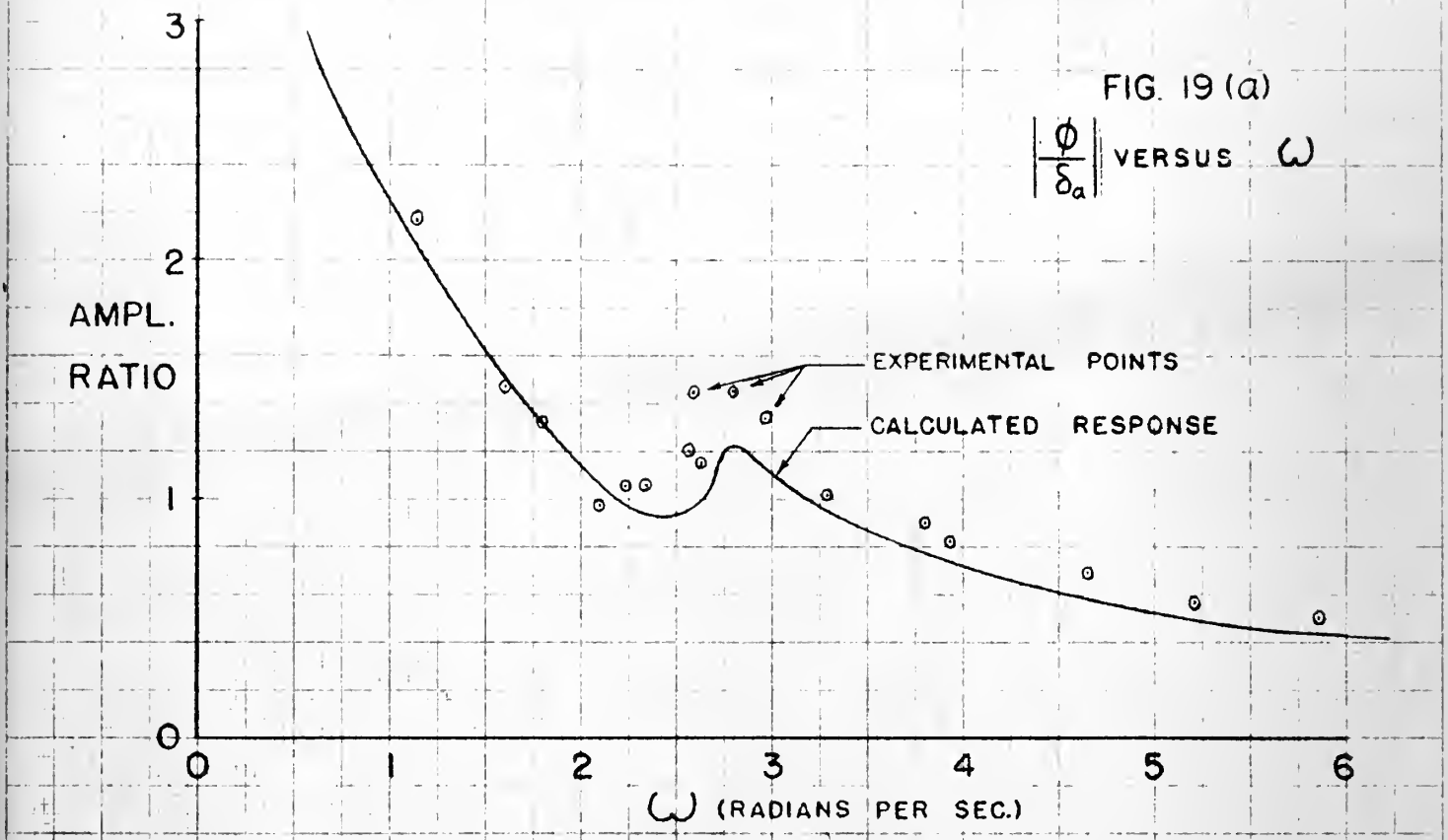

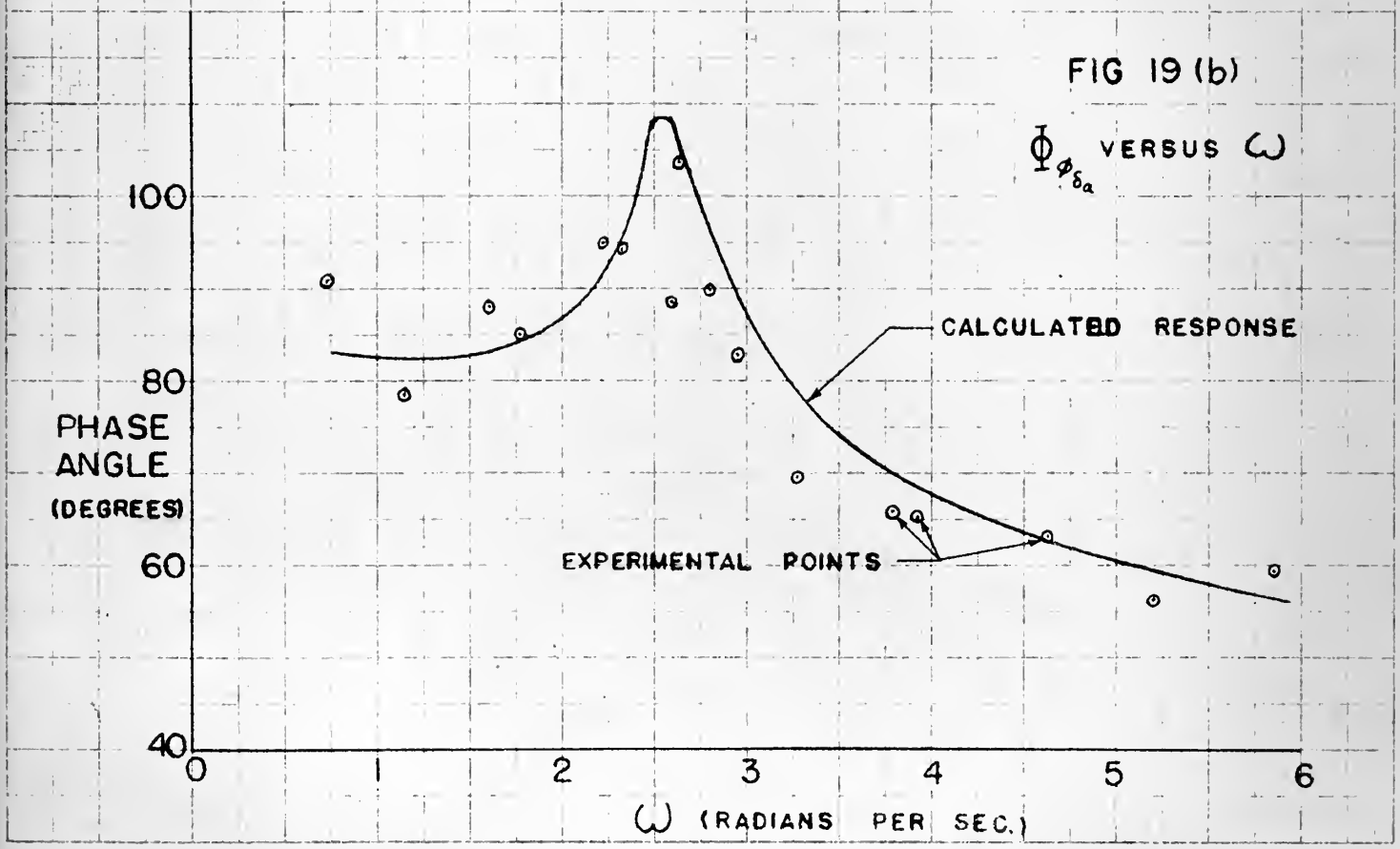

CALCULATED FREQUENCY RESPONSE IN YAW
FROM EXPERIMENTALLY DERIVED DERIVATIVES
TO AILERON OSCILLATIONS

FIG. 20(a)

$\left|\frac{\Psi}{\delta_a}\right|$ VERSUS ω

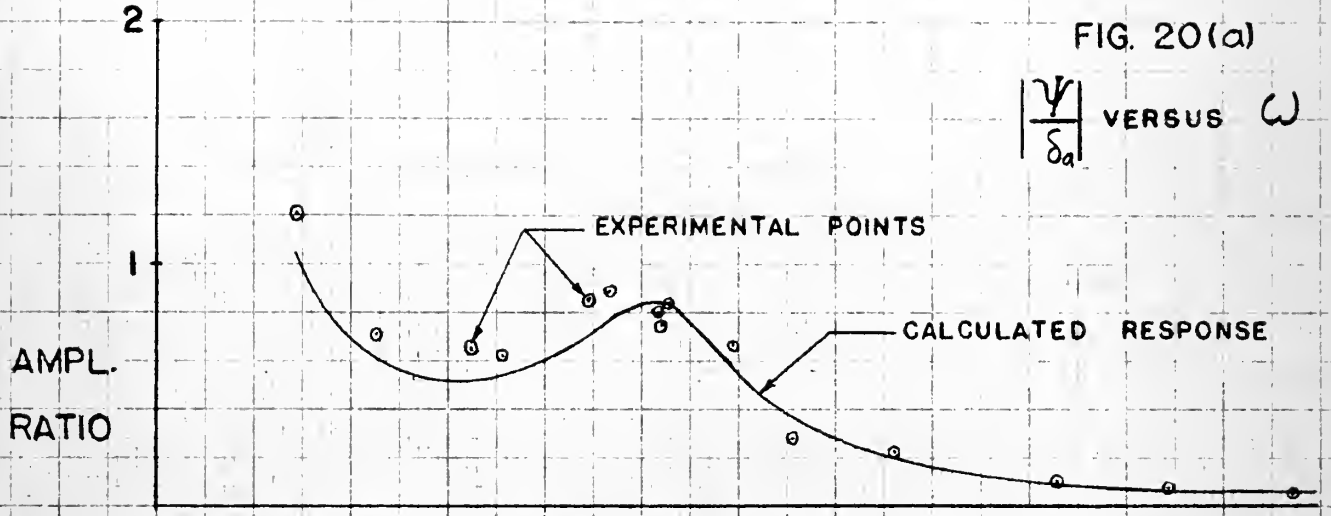

FIG. 20(b)

$\Phi_{\Psi_{\delta_a}}$ VERSUS ω

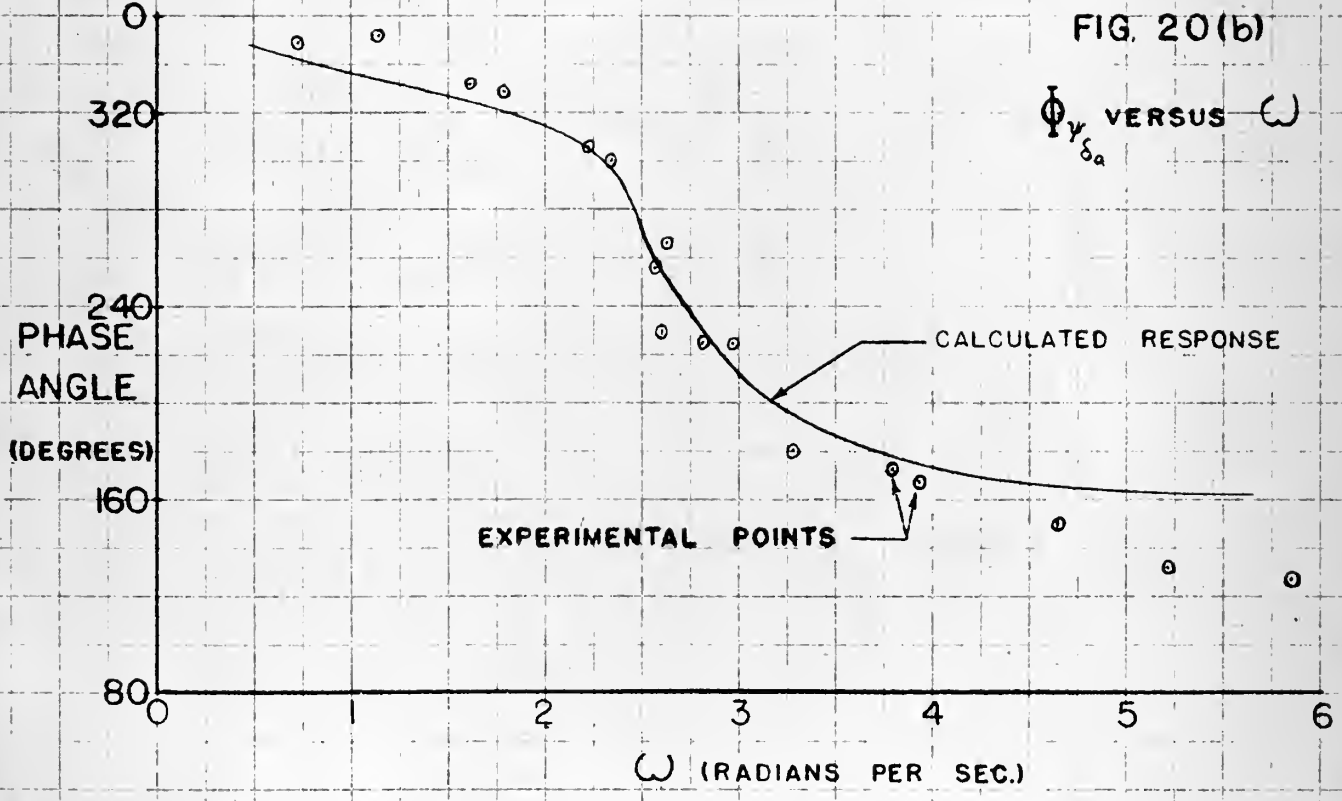

CALCULATED FREQUENCY RESPONSE IN SIDESLIP
FROM EXPERIMENTALLY DERIVED DERIVATIVES
TO AILERON OSCILLATIONS

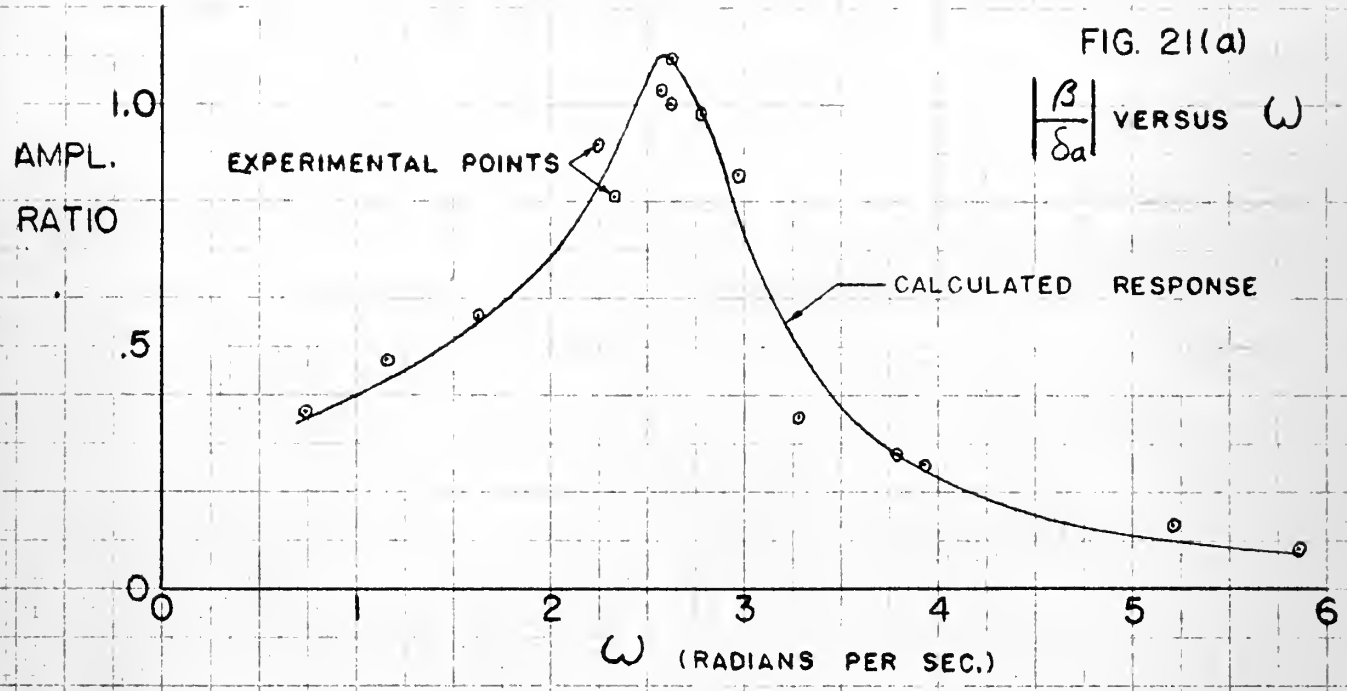

FIG. 21(a)

$\left|\frac{\beta}{\delta_a}\right|$ VERSUS ω

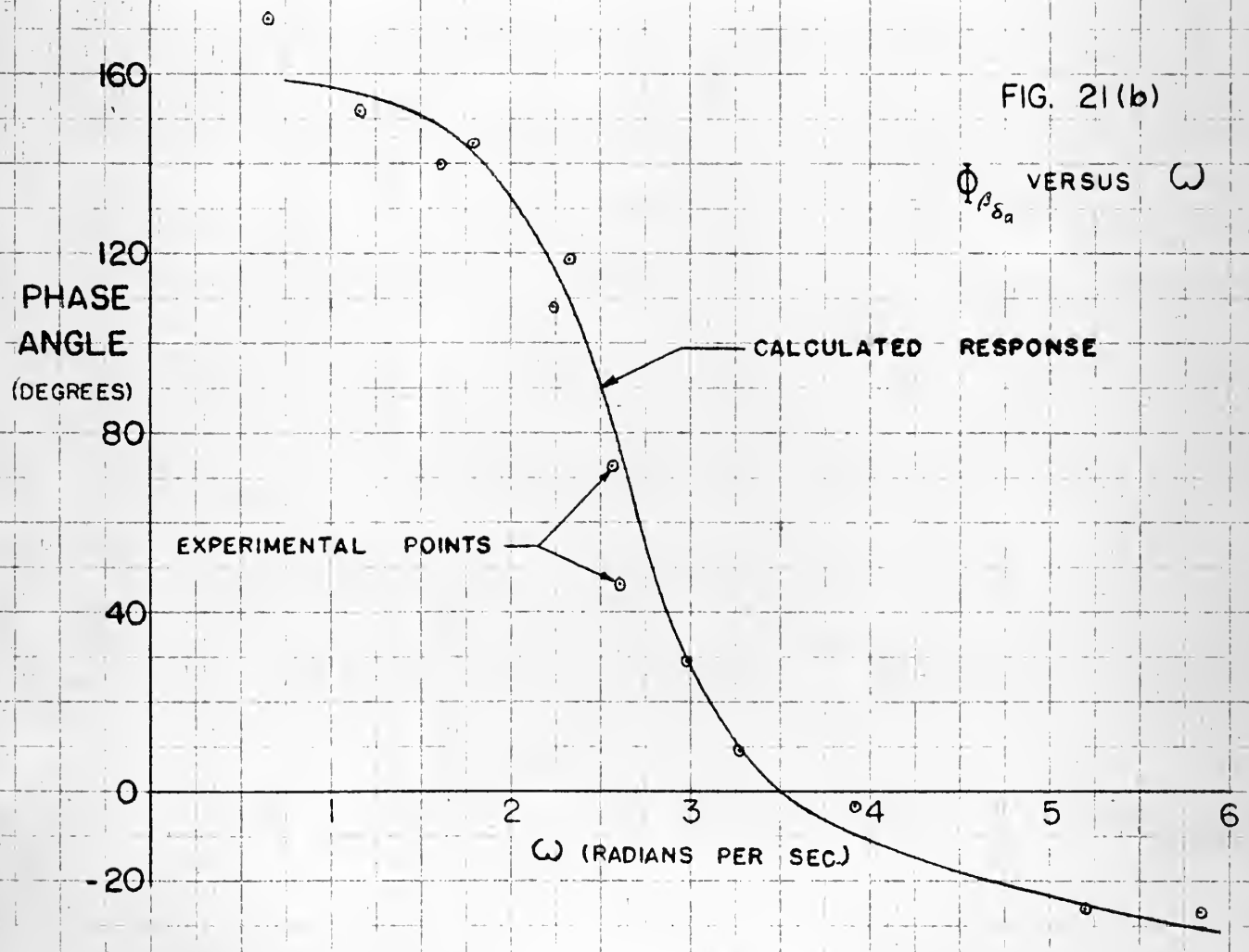

FIG. 21(b)

$\Phi_{\beta\delta_a}$ VERSUS ω

CALCULATED FREQUENCY RESPONSE IN ROLL
FROM EXPERIMENTALLY DERIVED DERIVATIVES
TO RUDDER OSCILLATIONS

FIG. 22 (a)

$\left|\frac{\phi}{\delta_r}\right|$ VERSUS ω

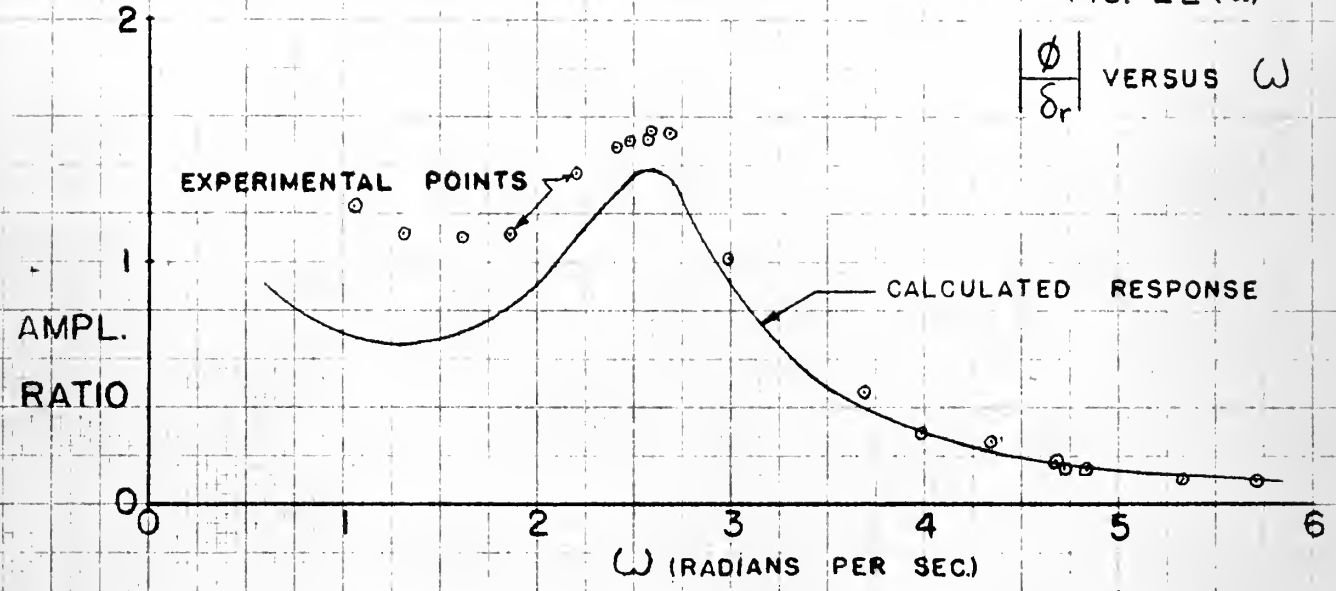

FIG. 22 (b)

$\Phi_{\phi_{\delta_r}}$ VERSUS ω

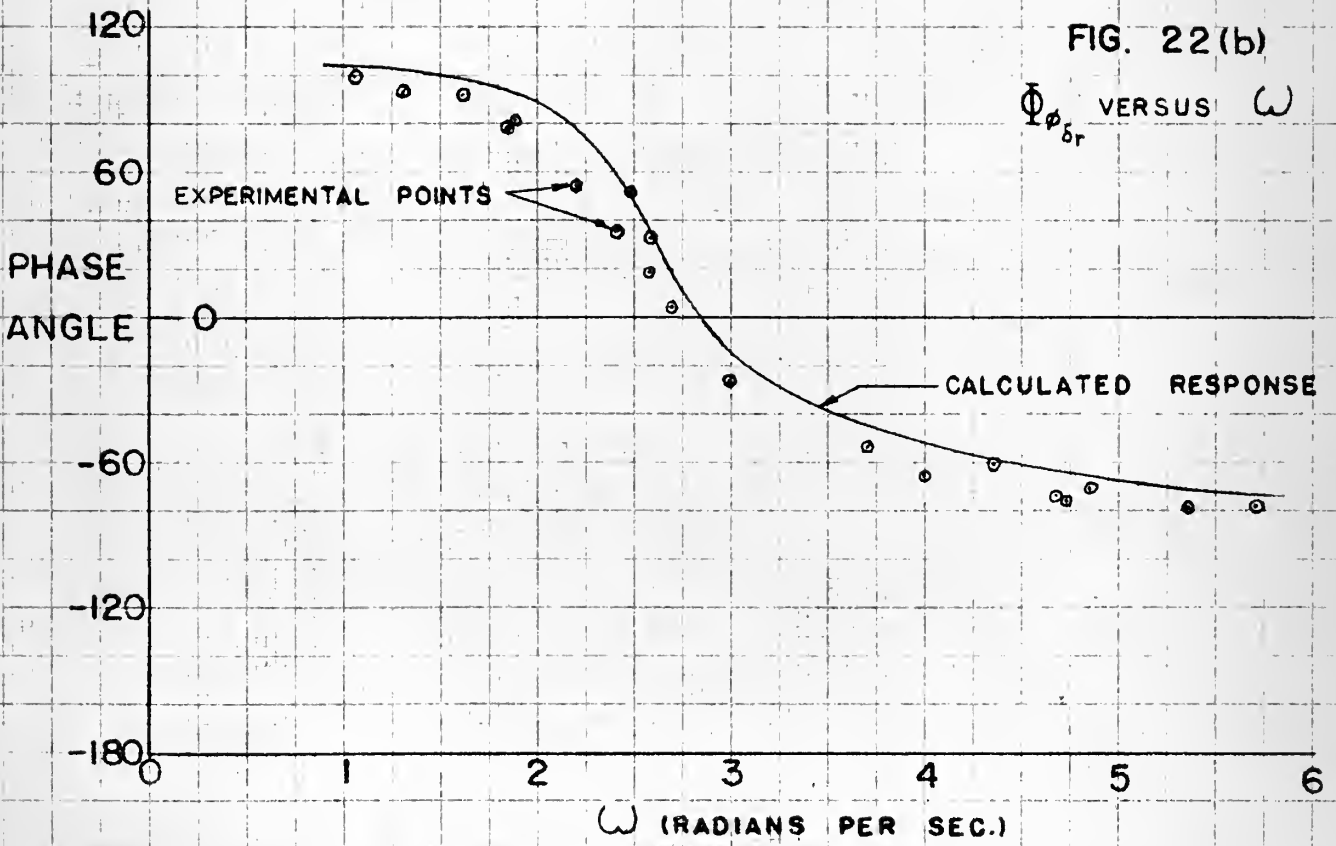

CALCULATED FREQUENCY RESPONSE IN YAW
FROM EXPERIMENTALLY DERIVED DERIVATIVES
TO RUDDER OSCILLATIONS

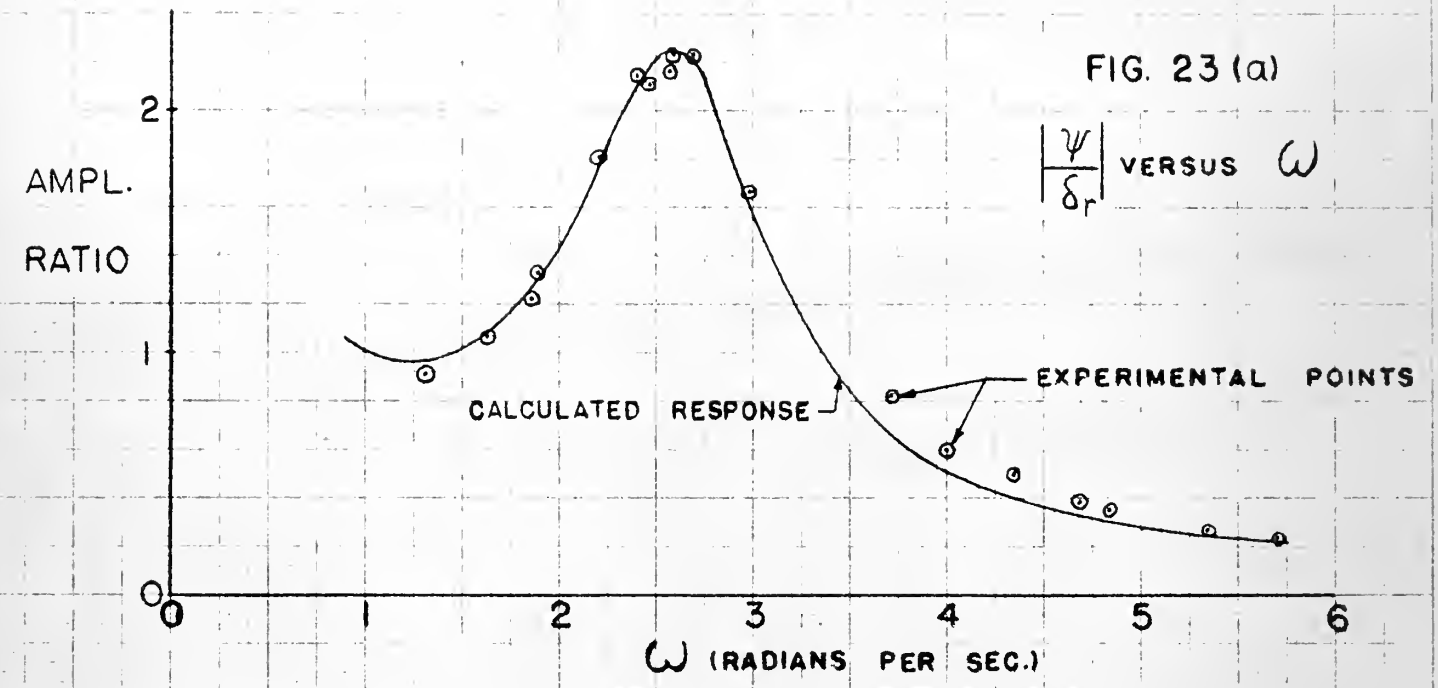

FIG. 23 (a)

$\left|\frac{\psi}{\delta_r}\right|$ VERSUS ω

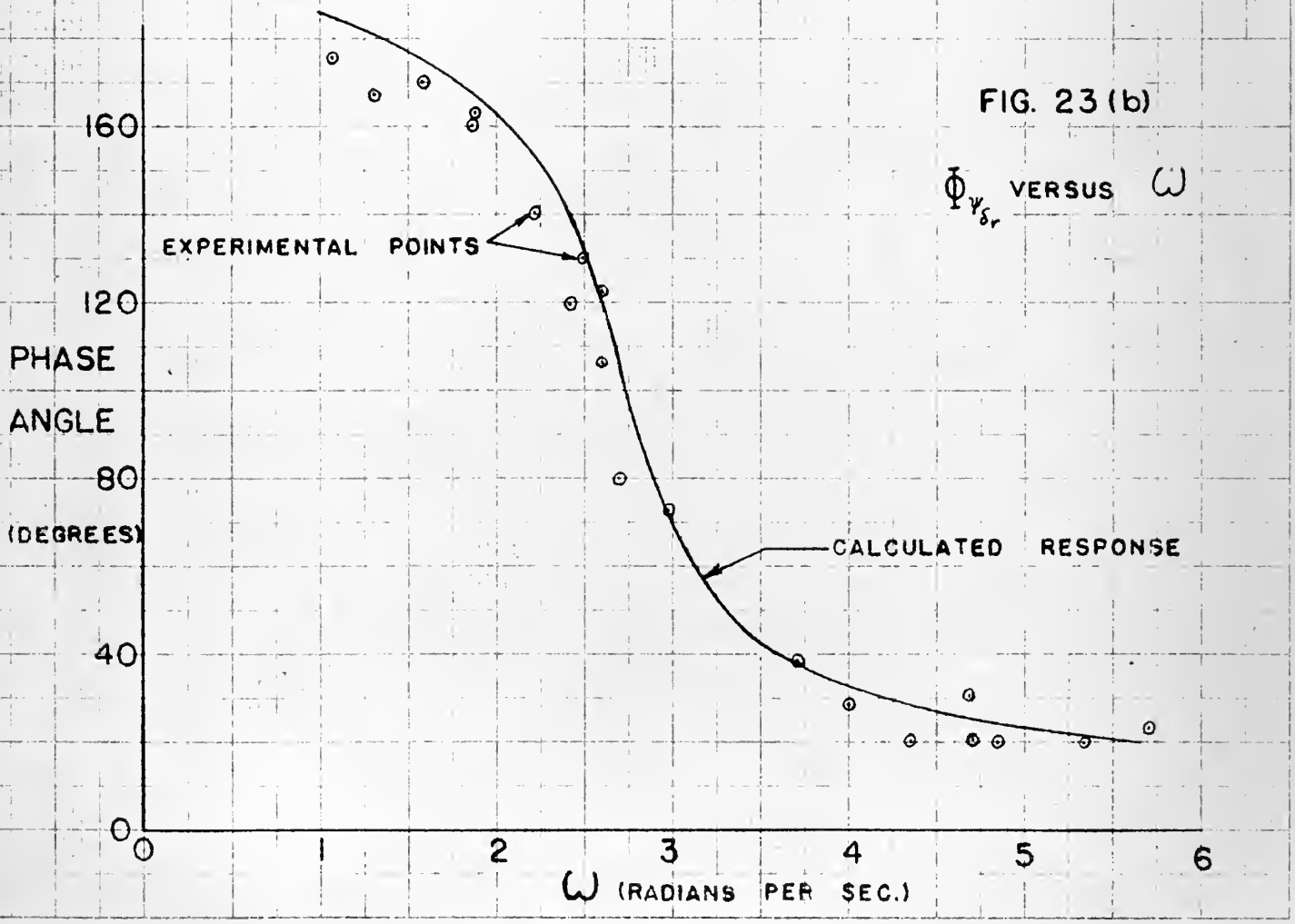

FIG. 23 (b)

$\Phi_{\psi_{\delta_r}}$ VERSUS ω

CALCULATED FREQUENCY RESPONSE IN SIDESLIP
FROM EXPERIMENTALLY DERIVED DERIVATIVES
TO RUDDER OSCILLATIONS

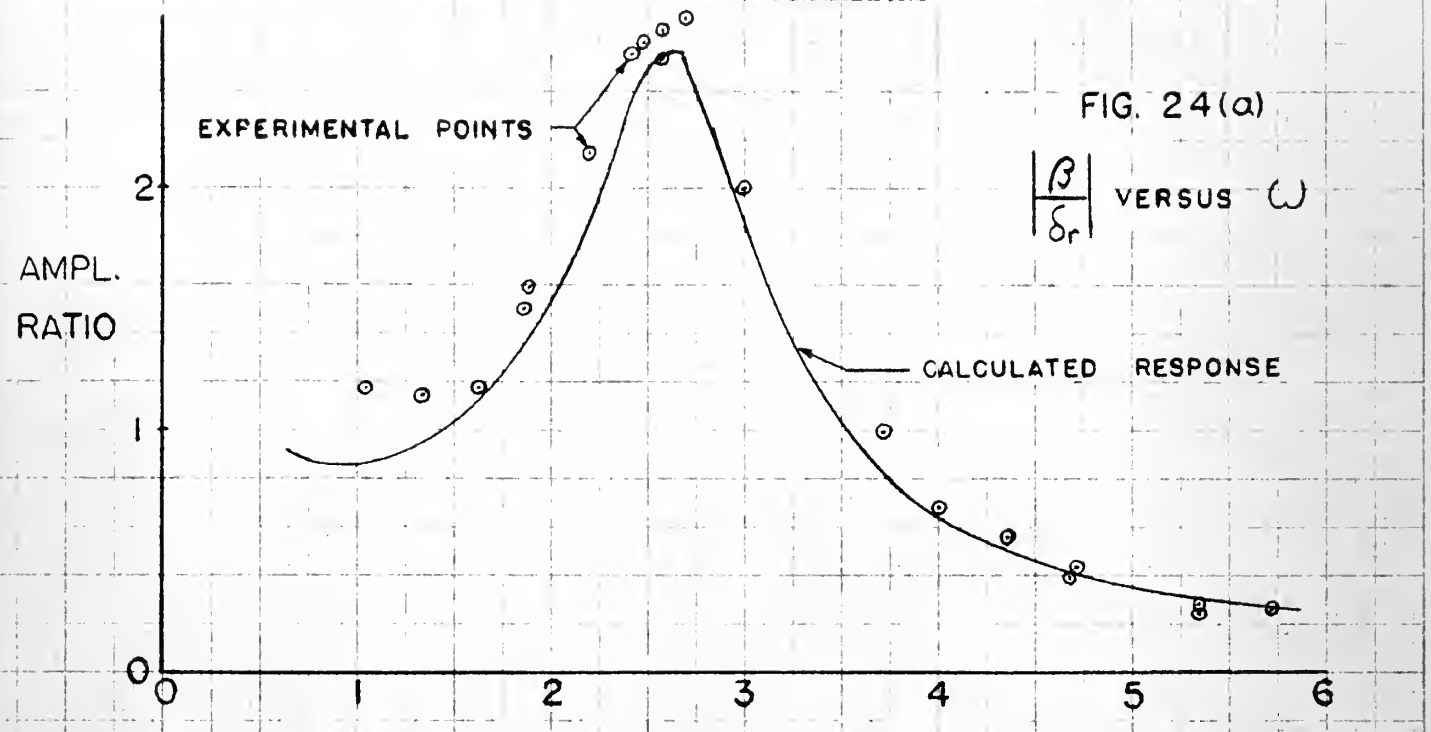

FIG. 24(a)

$\left|\frac{\beta}{\delta_r}\right|$ VERSUS ω

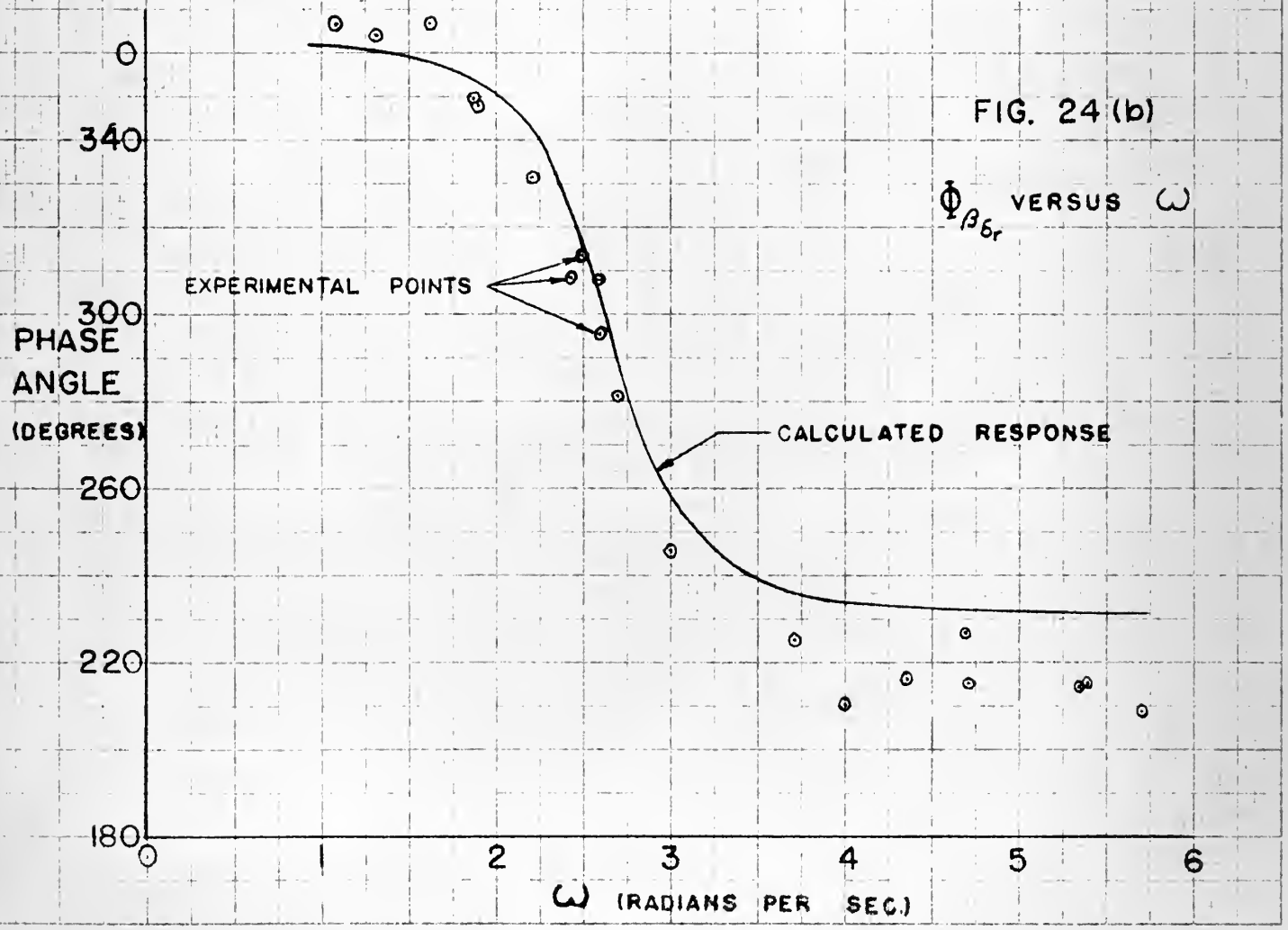

FIG. 24(b)

$\Phi_{\beta\delta_r}$ VERSUS ω

APPENDIX A

Development of Vector Equations of Lateral Motion for Determination of Stability Derivatives

The three linear equations of Lateral Motion may be written in the following form:

Side force: (1) $(D + C_{y_\beta}^*)\beta - C_L^* \phi + D\psi = C_{y_{\delta r}}^* \delta_r$

Roll: (2) $C_{\ell_\beta}^* \beta + (D^2 + C\ell_p^* D)\phi - \left(\frac{I_{xz}}{I_x} D^2 + C\ell_r^* D\right)\psi = C\ell_{\delta r}^* \delta_r + C\ell_{\delta a}^* \delta_a$

Yaw: (3) $-C_{n_\beta}^* \beta - \left(\frac{I_{xz}}{I_z} + C_{n_p}^* D\right)\phi + (D^2 + C_{n_r}^* D)\psi = C_{n_{\delta r}}^* \delta_r + C_{n_{\delta a}}^* \delta_a$

The coefficients of these equations are defined as follows:

$C_{y_\beta}^* = C_{y_\beta}\left(-\frac{1}{2T}\right)$

$C_L^* = C_L\left(\frac{1}{2T}\right) = g/V$

$C_{l_\beta}^* = C_{l_\beta}\left(-\frac{\mu}{J_x T^2}\right)$

$C_{l_p}^* = C_{l_p}\left(-\frac{1}{2J_x T}\right)$

$C_{l_r}^* = C_{l_r}\left(\frac{1}{2J_x T}\right)$

$C_{n_\beta}^* = C_{n_\beta}\left(\frac{\mu}{J_z T^2}\right)$

$C_{n_p}^* = C_{n_p}\left(\frac{1}{2J_z T}\right)$

$C_{n_r}^* = C_{n_r}\left(-\frac{1}{2J_z T}\right)$

$C_{y_{\delta r}}^* = C_{y_{\delta r}}\left(\frac{1}{2T}\right)$

$C_{l_{\delta r}}^* = C_{l_{\delta r}}\left(\frac{\mu}{J_x T^2}\right)$

$C_{n_{\delta r}}^* = C_{n_{\delta r}}\left(\frac{\mu}{J_z T^2}\right)$

$C_{l_{\delta a}}^* = C_{l_{\delta a}}\left(\frac{\mu}{J_x T^2}\right)$

$C_{n_{\delta a}}^* = C_{n_{\delta a}}\left(\frac{\mu}{J_z T^2}\right)$

The vector technique is applied to the equations in the following manner. If an input δ_r to a linear system is considered to have a sinusoidal variation of frequency ω, it can be considered to be a vector of unit magnitude lying along the real axis of the complex plane as shown in the sketch below.

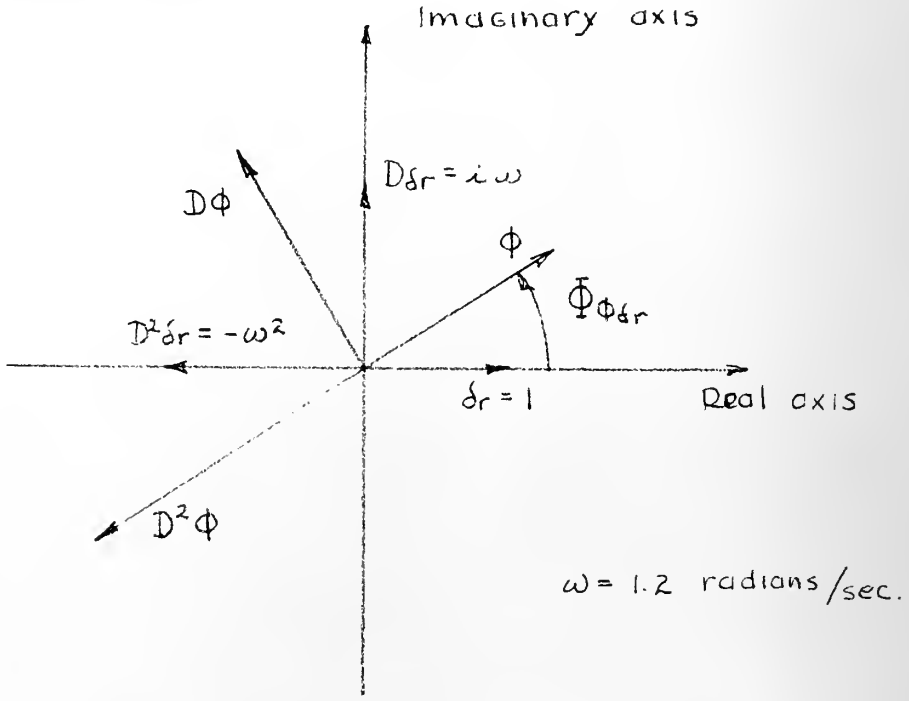

The first derivative of the sinusoidal input is obtained by multiplying amplitude by ω and rotating the vector through 90°. The steady state response of the system may be considered as a vector of amplitude ratio R and having a direction displaced from the real axis by a phase angle, Φ. Thus, in the complex plane, the vector for sideslip may represented as

$$\beta = \left|\frac{\beta}{\delta_r}\right| e^{i\Phi_{\beta\delta_r}} = \left|\frac{\beta}{\delta_r}\right| \left(\cos\Phi_{\beta\delta_r} + i \sin\Phi_{\beta\delta_r}\right) = A_\beta + i B_\beta$$

In complex notation the derivative of either the control input or the response for the steady state condition may be determined by multiplying by $i\omega$ and the integral by dividing by $i\omega$.

The following are defined:

$$A_\beta = \left|\frac{\beta}{\delta_r}\right| \cos \Phi_{\beta\delta r} \qquad B_\beta = \left|\frac{\beta}{\delta r}\right| \sin \Phi_{\beta\delta r}$$

$$A_\psi = \left|\frac{\psi}{\delta r}\right| \cos \Phi_{\psi\delta r} \qquad B_\psi = \left|\frac{\psi}{\delta r}\right| \sin \Phi_{\psi\delta r}$$

$$A_\phi = \left|\frac{\Phi}{\delta r}\right| \cos \Phi_{\phi\delta r} \qquad B_\phi = \left|\frac{\Phi}{\delta r}\right| \sin \Phi_{\phi\delta r}$$

In this notation with the input vector having a magnitude of unity the responses and their derivatives may be defined as follows:

(4) $\beta = A_\beta + i B_\beta$

(5) $D\beta = -\omega B_\beta + i\omega A_\beta$

(6) $D^2\beta = -\omega^2 A_\beta - i\omega^2 B_\beta$

(7) $\phi = A_\phi + i B_\phi$

(8) $D\Phi = -\omega B_\phi + i\omega A_\phi$

(9) $D^2\Phi = -\omega^2 A_\phi - i\omega^2 B_\phi$

(10) $\psi = A_\psi + i B_\psi$

(11) $D\psi = -\omega B_\psi + i\omega A_\psi$

(12) $D^2\psi = -\omega^2 A_\psi - i\omega^2 B_\psi$

Substitution of equations (4) to (12) in equations (1), (2), and (3) and separation into real and imaginary parts yields the following six simplified equations:

Sideforce: (13) $C_{y_\beta}^{*} B_\beta - C_L^{*} B_\phi = -\omega(A_\beta + A_\psi)$

(14) $C_{y_\beta}^{*} A_\beta - C_L^{*} A_\phi = C_{y_{\delta_r}}^{*} + \omega(B_\beta + B_\psi)$

Roll: (15) $C_{\ell_\beta}^{*} B_\beta + C_{\ell_p}^{*} \omega A_\phi + \frac{I_{xz}}{I_x}\omega^2 B_\psi - C_{\ell_r}^{*} \omega A_\psi = \omega^2 B_\phi$

(16) $C_{\ell_\beta}^{*} A_\beta - C_{\ell_p}^{*} \omega B_\phi + \frac{I_{xz}}{I_x}\omega^2 A_\psi + C_{\ell_r}^{*} \omega B_\psi - C_{\ell_{\delta_r}}^{*} = \omega^2 A_\phi$

Yaw: (17) $-C_{n_\beta}^{*} B_\beta - C_{n_p}^{*} \omega A_\phi + \frac{I_{xz}}{I_z}\omega^2 B_\phi + C_{n_r}^{*} \omega A_\psi = \omega^2 B_\psi$

(18) $-C_{n_\beta}^{*} A_\beta + C_{n_p}^{*} \omega B_\phi + \frac{I_{xz}}{I_z}\omega^2 A_\phi - C_{n_r}^{*} \omega B_\psi - C_{n_{\delta_r}}^{*} = \omega^2 A_\psi$

In these equations the A's and B's will be available from the frequency response curves for any chosen value of ω. In theory it is seen that equation (13) may be solved for $C_{y_\beta}^{*}$ from the response at a single frequency since C_L^{*} is known. Equation (14) may then be solved for $C_{y_{\delta_r}}^{*}$ using the computed value $C_{y_\beta}{}^{*}$. The complete solution of the yaw and roll equations may be accomplished if the responses are known at three different frequencies since the maximum number of unknown coefficients in any one equation never exceeds three. The method of averages attempts to eliminate random error in single points by writing each equation for a number of frequencies and grouping the equations thus determined in as many groups as there are unknowns. The coefficients for each group are summed and the resulting simultaneous equations are solved for the unknowns.

In the roll and yaw equations it is found that better solutions are

obtained if the grouping of points is performed in such a manner that all the points in a given group lie in the same frequency range and further that the three groups chosen include data below, at, and above the dutch roll frequency.

The final computational equations then become:

Side force: (19) $$C_{Y_\beta}^* \sum_1^{\omega_n} B_\beta - C_L^* \sum_1^{\omega_n} B_\Phi = -\sum_1^{\omega_n} \omega (A_\beta + A_\psi)$$

(20) $$C_{Y_\beta}^* \sum_1^{\omega_n} A_\beta - C_L^* \sum_1^{\omega_n} A_\Phi = n\, C_{Y_{\delta r}}^* + \sum_1^{\omega_n} \omega (B_\beta + B_\psi)$$

Roll: (21a) $$C_{\ell_\beta}^* \sum_1^{\omega_\ell} B_\beta + C_{\ell_p}^* \sum_1^{\omega_\ell} \omega A_\Phi + \frac{I_{xz}}{I_x} \sum_1^{\omega_\ell} \omega^2 B_\psi - C_{\ell_r}^* \sum_1^{\omega_\ell} \omega A_\psi = \sum_1^{\omega_\ell} \omega^2 B_\Phi$$

(21b) $$C_{\ell_\beta}^* \sum_{\omega_\ell}^{\omega_m} B_\beta + C_{\ell_p}^* \sum_{\omega_\ell}^{\omega_m} \omega A_\Phi + \frac{I_{xz}}{I_x} \sum_{\omega_\ell}^{\omega_m} \omega^2 B_\psi - C_{\ell_r}^* \sum_{\omega_\ell}^{\omega_m} \omega A_\psi = \sum_{\omega_\ell}^{\omega_m} \omega^2 B_\Phi$$

(21c) $$C_{\ell_\beta}^* \sum_{\omega_m}^{\omega_n} B_\beta + C_{\ell_p}^* \sum_{\omega_m}^{\omega_n} \omega A_\Phi + \frac{I_{xz}}{I_x} \sum_{\omega_m}^{\omega_n} \omega^2 B_\psi - C_{\ell_r}^* \sum_{\omega_m}^{\omega_n} \omega A_\psi = \sum_{\omega_m}^{\omega_n} \omega^2 B_\Phi$$

(22) $$C_{\ell_\beta}^* \sum_1^{\omega_n} A_\beta - C_{\ell_p}^* \sum_1^{\omega_n} \omega B_\Phi + \frac{I_{xz}}{I_x} \sum_1^{\omega_n} \omega^2 A_\psi + C_{\ell_r}^* \sum_1^{\omega_n} \omega B_\psi - n C_{\ell_{\delta r}}^* = \sum_1^{\omega_n} \omega^2 A_\Phi$$

Yaw: (23a) $$-C_{n_\beta}^* \sum_1^{\omega_\ell} B_\beta - C_{n_p}^* \sum_1^{\omega_\ell} \omega A_\Phi + \frac{I_{xz}}{I_z} \sum_1^{\omega_\ell} \omega^2 B_\Phi + C_{n_r}^* \sum_1^{\omega_\ell} \omega A_\psi = \sum_1^{\omega_\ell} \omega^2 B_\psi$$

(23b) $$-C_{n_\beta}^* \sum_{\omega_\ell}^{\omega_m} B_\beta - C_{n_p}^* \sum_{\omega_\ell}^{\omega_m} \omega A_\Phi + \frac{I_{xz}}{I_z} \sum_{\omega_\ell}^{\omega_m} \omega^2 B_\Phi + C_{n_r}^* \sum_{\omega_\ell}^{\omega_m} \omega A_\psi = \sum_{\omega_\ell}^{\omega_m} \omega^2 B_\psi$$

(23c) $$-C_{n_\beta}^* \sum_{\omega_m}^{\omega_n} B_\beta - C_{n_p}^* \sum_{\omega_m}^{\omega_n} \omega A_\Phi + \frac{I_{xz}}{I_z} \sum_{\omega_m}^{\omega_n} \omega^2 B_\Phi + C_{n_r}^* \sum_{\omega_m}^{\omega_n} \omega A_\psi = \sum_{\omega_m}^{\omega_n} \omega^2 B_\psi$$

(24) $$-C_{n_\beta}^* \sum_1^{\omega_n} A_\beta + C_{n_p}^* \sum_1^{\omega_n} \omega B_\Phi + \frac{I_{xz}}{I_z} \sum_1^{\omega_n} \omega^2 A_\Phi - C_{n_r}^* \sum_1^{\omega_n} \omega B_\psi - n C_{n_{\delta r}}^* = \sum_1^{\omega_n} \omega^2 A_\psi$$

The development of the computational equations was performed for the rudder case with the coefficients $C_{l_{\delta_a}}^*$ and $C_{n_{\delta_a}}^*$ equal to zero. It is obvious that for the aileron case the equations are identical to those developed above, with the substitution of $C_{l_{\delta_a}}^*$ and $C_{n_{\delta_a}}^*$ for $C_{l_{\delta_r}}^*$ and $C_{n_{\delta_r}}^*$ and $C_{y_{\delta_r}}^* = 0$.

If difficulty in the solution of the equations arises because of ill-conditioning, it may be possible to resolve in some direction other than that of the control deflection vector. It may also be possible to eliminate some troublesome coefficient between equations and thus obtain solutions. No attempt was made here to consider all the possibilities of modification of the equations.

If the derivatives are known, the transfer function coefficients may be easily developed as follows:

$$\frac{\beta}{\delta_r} = \frac{\begin{vmatrix} C_{Y_{\delta_r}}^* & -C_L^* & s \\ C_{l_{\delta_r}}^* & s^2 + C_{l_p}^* s & s^2 \frac{I_{xz}}{I_x} + C_{l_r}^* s \\ C_{n_{\delta_r}}^* & -\frac{I_{xz}}{I_z} s^2 - C_{n_p}^* s & s^2 + C_{n_r}^* s \end{vmatrix}}{\begin{vmatrix} s + C_{Y_\beta}^* & -C_L^* & s \\ C_{l_\beta}^* & s^2 + C_{l_p}^* s & \frac{I_{xz}}{I_x} s^2 + C_{l_r}^* s \\ -C_{n_\beta}^* & -\frac{I_{xz}}{I_z} s^2 - C_{n_p}^* s & s^2 + C_{n_r}^* s \end{vmatrix}}$$

$$\frac{\beta}{\delta_r} = \frac{C_5 s^3 + C_6 s^2 + C_7 s + C_8}{s^4 + C_1 s^3 + C_2 s^2 + C_3 s + C_4}$$

$$\frac{\Phi}{\delta r} = \frac{\begin{vmatrix} s + C_{Y_\beta}^{\star} & C_{Y_{\delta r}}^{\star} & s \\ C_{\ell_\beta}^{\star} & C_{\ell_{\delta r}}^{\star} & \frac{I_{xz}}{I_x} s^2 + C_{\ell_r}^{\star} s \\ -C_{n_\beta}^{\star} & C_{n_{\delta r}}^{\star} & s^2 + C_{n_r}^{\star} s \end{vmatrix}}{\begin{vmatrix} s + C_{Y_\beta}^{\star} & -C_L^{\star} & s \\ C_{\ell_\beta}^{\star} & s^2 + C_{\ell_p}^{\star} s & \frac{I_{xz}}{I_x} s^2 + C_{\ell_r}^{\star} s \\ -C_{n_\beta}^{\star} & -\frac{I_{xz}}{I_z} s^2 - C_{n_p}^{\star} s & s^2 + C_{n_r}^{\star} s \end{vmatrix}}$$

$$\frac{\Phi}{\delta r} = \frac{C_9 s^2 + C_{10} s + C_{11}}{s^4 + C_1 s^3 + C_2 s^2 + C_3 s + C_4}$$

$$\frac{\psi}{\delta r} = \frac{\begin{vmatrix} s + C_{Y_\beta}^{\star} & C_L^{\star} & C_{Y_{\delta r}}^{\star} \\ C_{\ell_\beta}^{\star} & s^2 + C_{\ell_p}^{\star} s & C_{\ell_{\delta r}}^{\star} \\ -C_{n_\beta}^{\star} & -\frac{I_{xz}}{I_z} s^2 - C_{n_p}^{\star} s & C_{n_{\delta r}}^{\star} \end{vmatrix}}{\begin{vmatrix} s + C_{Y_\beta}^{\star} & C_L^{\star} & s \\ C_{\ell_\beta}^{\star} & s^2 + C_{\ell_p}^{\star} s & \frac{I_{xz}}{I_x} s^2 + C_{\ell_r}^{\star} s \\ -C_{n_\beta}^{\star} & -\frac{I_{xz}}{I_z} s^2 - C_{n_p}^{\star} s & s^2 + C_{n_r}^{\star} s \end{vmatrix}}$$

$$\frac{\psi}{\delta r} = \frac{C_{12} s^3 + C_{13} s^2 + C_{14} s + C_{15}}{s\left(s^4 + C_1 s^3 + C_2 s^2 + C_3 s + C_4\right)}$$

The coefficients of the transfer functions are determined as follows, where $C_n = \frac{C'_n}{C'_0}$.

$$C_0' = 1 - \frac{(I_{xz})^2}{I_x I_z}$$

$$C_1' = C_{y_\beta}^* + C_{\ell_p}^* + C_{n_r}^* - C_{\ell_\beta}^* C_{n_p}^* - C_{\ell_r}^* \frac{I_{xz}}{I_z} - C_{Y_\beta}^* \frac{(I_{xz})^2}{I_x I_z}$$

$$C_2' = C_{n_\beta}^* + C_{Y_\beta}^* C_{\ell_p}^* + C_{Y_\beta}^* C_{n_r}^* + C_{\ell_p}^* C_{n_r}^* - C_{\ell_\beta}^* \frac{I_{xz}}{I_z} - C_{\ell_r}^* C_{n_p}^* - C_{Y_\beta}^* \frac{I_{xz}}{I_x} C_{n_p}^* - C_{Y_\beta}^* C_{\ell_r}^* \frac{I_{xz}}{I_z}$$

$$C_3' = C_L^* C_{\ell_\beta}^* + C_{\ell_p}^* C_{n_\beta}^* - C_{\ell_\beta}^* C_{n_p}^* + C_{Y_\beta}^* C_{\ell_p}^* C_{n_r}^* - C_{Y_\beta}^* C_{\ell_r}^* C_{n_p}^* - C_L^* \frac{I_{xz}}{I_x} C_{n_\beta}^*$$

$$C_4' = C_L^* C_{\ell_\beta}^* C_{n_r}^* - C_L^* C_{\ell_r}^* C_{n_\beta}^*$$

$$C_5' = C_{Y_{\delta r}}^* \left(1 - \frac{(I_{xz})^2}{I_x I_z}\right)$$

$$C_6' = C_{Y_{\delta r}}^* C_{\ell_p}^* + C_{Y_{\delta r}}^* C_{n_r}^* - \frac{I_{xz}}{I_z} C_{\ell_{\delta r}}^* - C_{n_{\delta r}}^* - C_{Y_{\delta r}}^* \frac{I_{xz}}{I_x} C_{n_p}^* - C_{Y_{\delta r}}^* C_{\ell_r}^* \frac{I_{xz}}{I_z}$$

$$C_7' = C_{Y_{\delta r}}^* C_{\ell_p}^* C_{n_r}^* - C_{\ell_{\delta r}}^* C_{n_p}^* + C_{n_{\delta r}}^* C_L^* \frac{I_{xz}}{I_x} - C_{n_{\delta r}}^* C_{\ell_p}^* + C_{\ell_{\delta r}}^* C_L^* - C_{Y_{\delta r}}^* C_{\ell_r}^* C_{n_p}^*$$

$$C_8' = C_{n_{\delta r}}^* C_L^* C_{\ell_r}^* + C_{\ell_{\delta r}}^* C_{n_r}^* C_L^*$$

$$C_9' = C_{\ell_{\delta r}}^* + C_{n_{\delta r}}^* \frac{I_{xz}}{I_x}$$

$$C_{10}' = C_{\ell_{\delta r}}^* C_{Y_\beta}^* + C_{Y_{\delta r}}^* \frac{I_{xz}}{I_x} C_{n_\beta}^* - C_{Y_{\delta r}}^* C_{\ell_\beta}^* + C_{n_{\delta r}}^* C_{\ell_r}^* + C_{n_{\delta r}}^* C_{Y_\beta}^* \frac{I_{xz}}{I_x} + C_{\ell_{\delta r}}^* C_{n_r}^*$$

$$C_{11}' = C\ell_{\delta r}^{*} C_{Y\beta}^{*} C_{nr}^{*} + C_{Y\delta r}^{*} C\ell_{r}^{*} C_{n\beta}^{*} + C_{n\delta r}^{*} C\ell_{\beta}^{*} + C\ell_{\delta r}^{*} C_{n\beta}^{*}$$
$$- C_{Y\delta r}^{*} C\ell_{\beta}^{*} C_{nr}^{*} + C_{n\delta r}^{*} C_{Y\beta}^{*} C\ell_{r}^{*}$$

$$C_{12}' = C_{n\delta r}^{*} + \frac{I_{xz}}{I_z} C\ell_{\delta r}^{*}$$

$$C_{13}' = C_{n\delta r}^{*} C\ell_{p}^{*} + C_{n\delta r}^{*} C_{Y\beta}^{*} - C_{Y\delta r}^{*} C\ell_{\beta}^{*} \frac{I_{xz}}{I_z} + C_{Y\delta r}^{*} C_{n\beta}^{*}$$
$$+ C\ell_{\delta r}^{*} C_{np}^{*} + C\ell_{\delta r}^{*} C_{Y\beta}^{*} \frac{I_{xz}}{I_z}$$

$$C_{14}' = C_{n\delta r}^{*} C_{Y\beta}^{*} C\ell_{p}^{*} - C_{Y\delta r}^{*} C\ell_{\beta}^{*} C_{np}^{*} + C_{Y\delta r}^{*} C\ell_{p}^{*} C_{n\beta}^{*}$$
$$+ C\ell_{\delta r}^{*} C_{Y\beta}^{*} C_{np}^{*}$$

$$C_{15}' = C\ell_{\delta r}^{*} C_{L}^{*} C_{n\beta}^{*} + C_{n\delta r}^{*} C_{L}^{*} C\ell_{\beta}^{*}$$

Once the transfer function coefficients are known the frequency response may be determined by the substitution of $i\omega$ for s, giving the following:

$$\left|\frac{\beta}{\delta_r}\right| = \sqrt{\frac{(C_8 + C_6\omega^2)^2 + (C_7\omega - C_5\omega^3)^2}{(\omega^4 - C_2\omega^2 + C_4)^2 + (C_3\omega - C_1\omega^3)^2}}$$

$$\Phi_{\beta\delta r} = \tan^{-1}\left(\frac{C_7\omega - C_5\omega^3}{C_8 - C_6\omega^2}\right) - \tan^{-1}\left(\frac{C_3\omega - C_1\omega^3}{\omega^4 - C_2\omega^2 + C_4}\right)$$

$$\left|\frac{\Phi}{\delta_r}\right| = \sqrt{\frac{(C_{11} - C_9\omega^2)^2 + (C_{10}\omega)^2}{(\omega^4 - C_2\omega^2 + C_4)^2 + (C_3\omega - C_1\omega^3)^2}}$$

$$\Phi_{\Phi\delta r} = \tan^{-1}\left(\frac{C_{10}\omega}{C_{11} - C_9\omega^2}\right) - \tan^{-1}\left(\frac{C_3\omega - C_1\omega^3}{\omega^4 - C_2\omega^2 + C_4}\right)$$

$$\left|\frac{\psi}{\delta_r}\right| = \sqrt{\frac{\left(C_{15} - C_{13}\omega^2\right)^2 + \left(C_{14}\omega - C_{12}\omega^3\right)^2}{\left(C_1\omega^4 - C_3\omega^2\right)^2 + \left(\omega^5 - C_2\omega^3 + C_4\omega\right)^2}}$$

$$\Phi_{\psi_{\delta r}} = \tan^{-1}\left(\frac{C_{14}\omega - C_{12}\omega^3}{C_{15} - C_{13}\omega^2}\right) - \tan^{-1}\left(\frac{\omega^5 - C_2\omega^3 - C_4\omega}{C_1\omega^4 - C_3\omega^2}\right)$$